The Journal of Experimental Biology 200, 1661–1680 (1997)
Printed in Great Britain © The Company of Biologists Limited 1997
JEB0870

LARVAL LOCOMOTION OF THE LANCELET *BRANCHIOSTOMA FLORIDAE*

M. DALE STOKES*
Hopkins Marine Station, Stanford University, Pacific Grove, CA 93950, USA

Accepted 24 March 1997

Summary

The ontogeny of locomotion in the Florida lancelet (*Branchiostoma floridae*) is described for the early developmental stages through to metamorphosis. Recently hatched larvae swam at speeds up to 1 mm s^{-1} using their epidermal cilia; this speed decreased to approximately 0.2 mm s^{-1} by 60 h after fertilization. Changes in cilia-powered fluid flow could be related to changes in the distribution and density of the epidermal cilia during development. Cilia-powered hovering was the dominant behaviour until metamorphosis. The amount of energy expended by ciliating larvae ranged from 10^{-9} to 10^{-11} W depending upon the age of the larvae and the model used for estimating the power output. The majority of the energy expended was in the ciliary sublayer next to the body. The first muscular movements were seen in larvae 16 h old. These simple flexions increased in complexity during the first 72 h until a complete undulatory (approximately sinusoidal) wave was propagated down the body in the adult manner. The frequency of undulatory beating increased to approximately 10 Hz during the first 48 h, and the larval head showed a large degree of yaw. Lancelet larvae were also capable of high-speed undulations 5–10 times faster than regular swimming motions. In contrast to ciliating larvae, the energy expended during undulation was at least an order of magnitude greater (10^{-8} to 10^{-6} W) and radiated beyond the ciliary sublayer.

Key words: lancelet, amphioxus, *Branchiostoma floridae*, locomotion, cilia, undulatory locomotion, ontogeny, swimming, larval development, cephalochordate.

Introduction

Lancelets (amphioxus) of the chordate subphylum Cephalochordata in the phylum Chordata are found in tropical and temperate oceans worldwide. Lancelet larvae, in particular, have played an important role in discussions considering the origin of the vertebrates from the invertebrates. During their development, lancelet larvae are capable of swimming using either their epidermal cilia or muscular body undulations, making them unique among pelagic larvae (Chia *et al.* 1984). The transition from ciliary to undulatory swimming figures prominently in many evolutionary scenarios of vertebrate origins (Garstang, 1928; Berill, 1955; Gutmann, 1981; Bergstrom, 1989; Gans, 1989, 1993; Fetcho, 1992; Lacalli, 1996). The lack of substantial data on the locomotory mechanics of amphioxus larvae has not gone unnoticed (e.g. Fetcho, 1992); however, the majority of phylogenetic scenarios still rely on anecdotal observations. Because of this, the ontogeny of locomotion in amphioxus is important both for its possible phylogenetic significance and also from a purely biomechanical viewpoint because undulatory swimming begins at a markedly smaller body size than in developing vertebrates.

The locomotion and neuromuscular mechanics of adult amphioxus have been studied previously. Webb (1973, 1975, 1976*a*) corrected some earlier, fanciful misconceptions and described swimming in adults of *Branchiostoma lanceolatum*, and the properties of the adult's muscular notochord have been reviewed by Guthrie (1975).

Speculation on the locomotion of lancelet larvae has generated a voluminous literature. However, most previous accounts of larval locomotion are anecdotal, based on only a few developmental stages, and are often contradictory. The ciliated locomotion of lancelet larvae was noted by Kowalevsky (1867) and Willey (1891, 1894), and muscular movements were first noted by Leuckart and Pagenstecher (1858), then by van Wijhe (1927) and Bone (1958), although authors have not agreed on the position of the larva in the water or the relative importance of undulatory swimming (see conflicting accounts in Willey, 1891; van Wijhe, 1925, 1927; Chin, 1941; Bone, 1958; Wickstead and Bone, 1959; Webb, 1969, 1975, 1976*a*; Wickstead, 1975). Stokes and Holland (1995*b*) have since shown that, in *B. floridae*, pre-metamorphic larvae are planktonic and their behaviour is dominated by cilia-powered hovering in the water column.

The purpose of this investigation was to study the kinematics

*e-mail: dstokes@leland.stanford.edu.

of both ciliary and undulatory swimming during development in *B. floridae*, as well as to characterize changes in body morphology, including the distribution and density of ciliated epidermal cells relevant to locomotion. Using this information, it was possible to make estimates of the amount of energy expended during larval swimming and to relate the ontogeny of locomotion to lancelet ecology and phylogeny. Because the ciliated sensory cells of post-metamorphic lancelets (Schulte and Riehl, 1977; Bone and Best, 1978; Baatrup, 1981; Stokes and Holland, 1995*a*) as well as the undulatory motion of lancelet adults have been studied elsewhere, this investigation concentrates on the developmental period between hatching and metamorphosis.

Materials and methods

Adults of *Branchiostoma floridae* (Hubbs) were collected from Old Tampa Bay, Florida, USA, during the summer and spawned in the laboratory using the methods of Holland and Holland (1994). The subsequent embryonic and larval stages were raised through metamorphosis using the procedures outlined in Stokes and Holland (1995*a*,*b*).

Myotome number, cilia density and distribution

For scanning electron microscopy (SEM), samples of a few dozen developing lancelets were taken periodically from the culture (22.5 °C). Specimen fixation was in 2 % glutaraldehyde in filtered Tampa Bay water. The sample was then refrigerated (at 8 °C) until further processing. The fixed samples were washed for 2 min in distilled water, dehydrated in an ethanol series, critical-point dried by the CO_2 method (Stokes and Holland, 1995*a*), mounted on SEM stubs with double-sided tape, sputter-coated with a mixture of gold and palladium, and viewed using a Cambridge Instruments 360 scanning electron microscope. The epidermal surface of approximately 12 individuals from each sample was examined using SEM, and over 650 photomicrographs were made documenting changes in external morphology during lancelet ontogeny (see also Stokes and Holland, 1995*a*). Owing to the shrinkage of the lancelets during SEM preparation, the muscle myotomes were visible in larvae larger than 1 mm total length and their number was counted with reference to other concurrent ontogenetic events (e.g. the number of gill slits present).

In order to quantify the type, density and distribution/dispersion of epidermal cilia, 150 photomicrographs of post-hatching embryos and larvae at different developmental stages (i.e. 18, 24, 48, 96, 156, 204, 252, 420, 480 and 768 h post-hatching, as well as during metamorphosis) were analyzed further. On each, the number and type of ciliated cells within a ‘quadrate’ grid was counted. Between 10 and 50 quadrates (depending on the magnification of the micrograph and the density of the cilia present) were counted for each of several different quadrate sizes. The quadrate sizes were chosen such that the maximum number of cilia counted per quadrate was between three and nine, for effective tests of dispersion using contiguous quadrate methods (Pielou, 1974; Boots and Getis, 1988), but additional counts were made at half and twice the chosen quadrate size for comparison and as a test for sampling bias. The quadrate counts were then used to calculate average cilia densities for different body regions and were compared with a spatially random Poisson distribution using the *G*-statistic (Sokal and Rohlf, 1981). For those samples having a significant non-random distribution, an index of dispersion was calculated as the ratio of the sample variance to the sample mean (Grieg-Smith, 1957; Pielou, 1974; Boots and Getis, 1988) to indicate the degree to which cilia were uniformly distributed or clumped.

Video recordings

To observe swimming behaviour, sub-samples of the cultured lancelets (containing approximately 12–50 individuals, depending upon size and developmental stage), were placed in a small Petri dish (8 cm diameter, 12 mm deep) and video recordings were made from above for 20 min. In all cases, observations were made near the centre of the vessel to minimize wall effects. Video observations were made at 4 h intervals for the first 48 h after fertilization, at 24 h intervals for the next 10 days, and then at 72 h intervals until metamorphosis was complete. Two different camera systems were used for recording. A television camera (JVC model GXN4U) fitted with a Minolta macro lens (100 mm, *f*=4) permitted magnification to 50× and was used in conjunction with an external fibre-optic light source to provide dark-field illumination. In addition, an Olympus compound microscope, with an attached video camera (Sony model SSC-C350) and phase-contrast imaging, was used in conjunction with particles in the water (non-motile algae, *Isochrysis* sp.) to visualize fluid flow around the swimming lancelets. Once larvae exhibited mid-water hovering, they were also observed from the side in a larger (8 cm diameter, 6 cm deep) vessel (for details, see Stokes and Holland, 1995*b*). A small sample of larval and juvenile lancelets was also observed using a Kodak Ektapro high-speed video system (500 and 1000 frames s^{-1}). Relevant kinematic measurements were made from the recordings using a video monitor and after calibrating the camera systems using known size scales.

Newly hatched embryonic and larval lancelets swim through the water following a helical pathway similar to that of many ciliated protozoa. The helix appears as a sinusoidal curve when viewed in only two dimensions. By superimposing sequential video frames onto one image frame, the swimming pathways of motile lancelets could be analyzed and the path wavelength, amplitude and body radius measured. These parameters were then used to calculate the following kinematic components (Sugino and Naitoh, 1988; Sugino, 1993):

Path straightness (s):

$$s = \frac{\Gamma(t)}{\Gamma_p(t)}\ , \qquad (1)$$

where Γ_p is the swimming path length in time t, and Γ is the actual migration distance.

Forward swimming velocity (U):

$$U = \pm \frac{\sqrt{\lambda^2 + 4\pi^2\alpha^2}}{t_e}, \quad (2)$$

where λ is the swimming path wavelength, α is the path amplitude and t_e is the period of one helical cycle. Negative numbers indicate that the individual is swimming backwards (posterior end first). For those individuals not swimming using a helical pathway, the forward swimming velocity was calculated by dividing the distance travelled between successive points by the travel time.

At the onset of larval undulatory locomotion, the following kinematic components were measured from the superimposed video images: swimming speed, beat frequency, degree of head/tail yaw (measured as the maximum angle of deviation of the head and tail from the midline of the body during swimming), percentage of undulatory wave on the body, undulatory wavelength and amplitude.

Graphical representation of the flow field

To visualize the motion of water surrounding the swimming larvae, the positions of non-motile particles in the focal plane of the swimming larvae were traced over successive video frames to produce streaklines indicating the direction of fluid flow. In the case of cilia-powered swimming, particle velocities were also measured, allowing the contouring of flow speeds and a description of the flow field surrounding the larvae. To compare the fluid flow generated from ciliary *versus* undulatory processes graphically, vector diagrams were produced showing the change in relative particle position in a regular grid of points around the larva (81 or 162 points) over a 0.1 s interval.

For cilia-powered flow, positions were calculated from flow speeds and streaklines. However, for undulatory motion, flow diagrams of streaklines were not available owing to the complexity and speed of the motion. Instead, the relationship between net particle displacement and distance away from the undulating body was determined as an exponential decay function calculated from video analysis of particles moving around a stationary undulating body (larvae with heads fixed in place). The movement of hypothetical particles, which corresponded to positions on the regular grid, was then estimated by solving for the distance along a line from the particle to the surface of the larva normal to the surface of the body. Thus, the movement of each particle is an estimate of water movement rather than a direct measurement. This process was repeated to produce the differences in position for four sequential video fields for all 81 points. Where a single particle of water could be influenced by more than one line normal to the body (i.e. on the concave side of the bending body), the movement was estimated by calculating the average movement that results from several normals. Such measurements of the change in position of specific points occurring over a known period is a finite differencing technique and produces an estimate of the velocity vector field operating on the fluid (Happer and Brenner, 1983). The results are the product of applying this velocity field to the position data and represent both the fluid flow and the volume of fluid influenced by the motion of the undulating animal.

Estimation of locomotory power expenditure

To estimate the energy expended during locomotion, kinematic measurements from the video analysis were applied to several different theoretical models of swimming at low Reynolds number. U is the swimming speed, and η is the dynamic viscosity of water ($=0.9948\times10^{-3}$ Pa s at the laboratory culture temperature of 22.5 °C and at 20 ‰ salinity). Most of the models included surface area as one of the parameters and, in these cases, surface area was calculated as the surface area (S) of a prolate spheroid with semi-major and semi-minor axes (a and b respectively) measured from the radius and length of the larva:

$$S = 2\pi b^2 + \frac{\pi a^2 b}{\sqrt{a^2 - b^2}} \arcsin\frac{\sqrt{a^2 - b^2}}{a}. \quad (3)$$

Keller and Wu (1977) estimated ciliary power and defined the local flow field (outside the ciliary beat envelope) using a porous prolate model. The Stokes equations of fluid flow at low Reynolds number were solved to describe the fluid motion around an inert (i.e. sedimenting) and actively swimming body with the shape of a prolate spheroid.

For the inert and active body, the power P expended to maintain the flow field is:

$$P_{\text{inert}} = \frac{16\pi\eta a\varepsilon^3 U^2}{[(\delta + \varepsilon^2)L - 2\varepsilon]}, \quad (4)$$

and

$$P_{\text{active}} = \frac{8\pi\eta a[(\delta + \varepsilon^2)L - 2\varepsilon](\delta - 2)\varepsilon^3}{[2\varepsilon - (\delta - 2)L]^2}(U - V)^2. \quad (5)$$

In both cases, δ is the body length, ε is the eccentricity of the spheroid, $\varepsilon = \sqrt{a^2 - b^2}/a$, $L = \log[(1+\varepsilon)/(1-\varepsilon)]$ and V is the maximum suction velocity created by the cilia (V approaches zero in an ideal rigid (no slip) prolate spheroid moving parallel to its major axis). Additionally, using an average estimate of the energy expended per cilium (10^{-14} W) within the ciliary envelope (Keller and Wu, 1977), the average total power for all cilia was approximated from the density of cilia coverage and the larval surface area. Roberts (1981) also approximates the power expended within the ciliary envelope as (here expanded using the above formula for the surface area of a prolate spheroid, rather than the surface area of a sphere):

$$P = \frac{8\eta U^2}{\delta}\left[\pi b^2 + \frac{\pi a^2 b}{\sqrt{a^2 - b^2}} \arcsin\frac{\sqrt{a^2 - b^2}}{a}\right]. \quad (6)$$

Emlet (1994) estimated the force necessary to overcome viscous drag F_d for a 2:1 prolate spheroid (from Vogel, 1981) as:

$$F_d = C_v \eta S^{1/2} U, \quad (7)$$

where C_v is the viscous drag coefficient calculated from the

Stokes' law corrections in Happer and Brenner (1983), using a sphere of equivalent radius to the prolate spheroid of eccentricity and surface area closest to the larval form.

From this relationship, the power can be approximated by:

$$P = C_{\mathrm{v}}\eta S^{1/2}U^{2}. \quad (8)$$

The power expended during undulatory swimming *via* the body musculature was similarly estimated by a series of different models. In most instances, these models estimate power as a function of the undulatory wave speed (W), wavelength (λ), body length (δ), swimming speed (U) and the components of the viscous drag coefficients tangential and normal to the flow.

There has been debate over how to calculate viscous drag coefficients (see Azuma, 1992). In all instances, the coefficient is for an inclined cylinder of length δ (=body length) and diameter d, both normal ($C_{\mathrm{v,n}}$) and tangential ($C_{\mathrm{v,t}}$) to the fluid flow; however, different authors use different denominator constants, so power was calculated separately using the following coefficients from Gray and Hancock (1955):

$$C_{\mathrm{v,n}} = \frac{4\pi\eta}{\ln\left(\frac{4\lambda}{d}\right) - 0.5}$$

$$C_{\mathrm{v,t}} = \frac{2\pi\eta}{\ln\left(\frac{4\lambda}{d}\right) - 0.5}; \quad (9)$$

Lighthill (1976), Wu (1977), where constant q=0.09l:

$$C_{\mathrm{v,n}} = \frac{4\pi\eta}{\ln\left(\frac{4q}{d}\right) + 0.5}$$

$$C_{\mathrm{v,t}} = \frac{2\pi\eta}{\ln\left(\frac{4q}{d}\right) - 0.5}; \quad (10)$$

and Cox (1970):

$$C_{\mathrm{v,n}} = \frac{4\pi\eta}{\ln\left(\frac{\delta}{d}\right) + \ln 2 - 0.5}$$

$$C_{\mathrm{v,t}} = \frac{2\pi\eta}{\ln\left(\frac{\delta}{d}\right) + \ln 2 - 1.5}. \quad (11)$$

From these coefficients, the following estimates of undulatory power expenditure were used from Roberts (1981):

$$P = \delta C_{\mathrm{v,t}} W^{2}\left[\left(\frac{\lambda_{\mathrm{f}}}{\lambda}\right)^{2} - 1 + \frac{U}{W}\right], \quad (12)$$

where

$$\lambda_{\mathrm{f}} \cong \lambda\left(1 + \frac{2\pi^{2}b^{2}}{\lambda^{2}}\right)^{1/2}; \quad (13)$$

and from Azuma (1992):

$$P = \int(\mathrm{d}D_{\mathrm{t}}U_{\mathrm{t}} + \mathrm{d}D_{\mathrm{n}}U_{\mathrm{n}}), \quad (14)$$

where D_{t}, D_{n} and U_{t}, U_{n} are the drag and body segment velocity tangential and normal to the direction of motion, respectively. This equation has been solved for undulation including helical motion or remaining strictly planar. The lengthy algebraic expansion for planar undulation can be found in Azuma (1992). The expansion for helical undulatory power is:

$$P = C_{\mathrm{v,n}}W^{2}n\Lambda\frac{\left\{\left[\left(1 \pm \frac{U}{W}\right)^{2}\left(\frac{2\pi\omega}{\lambda}\right)^{2} + \frac{C_{\mathrm{v,t}}}{C_{\mathrm{v,n}}}\left[\frac{U}{W} + \left(\frac{2\pi\omega}{\lambda}\right)^{2}\right]^{2}\right\}}{\left[1 + \left(\frac{2\pi\omega}{\lambda}\right)^{2}\right]}, \quad (15)$$

where

$$\Lambda = \lambda\sqrt{1 + \left(\frac{2\pi\omega}{\lambda}\right)^{2}}, \quad (16)$$

n is the number of waves along the body and ω is the amplitude of the undulation.

Results

External morphology: myotomes and cilia

As lancelets grow, the number of myotomes increases from approximately four at the time of hatching (12 h after fertilization) to the full complement of approximately 60 in the adult (Fig. 1). Larvae less than approximately 1 mm long and without gill slits had fewer than 10 myotomes. Older, larger larvae showed a steady increase in myotome number and body length (see Fig. 3B) until metamorphosis (after the formation of 11 gill slits and the atrium that further encloses them, at approximately 960 h of development at laboratory temperature), at which point the number of myotomes no longer increased.

Motile cilia, approximately 10 μm in length, are found at uniform density over the entire larval surface for approximately the first 24 h after fertilization at a density of approximately 6 cilia per 100 $\mu\mathrm{m}^{2}$ (Fig. 2). Older larvae show a decrease in motile cilia density until metamorphosis (after which it becomes hard to distinguish cilia externally in micrographs owing to a covering of mucus on the body surface). The loss of motile cilia does not occur at a constant rate over the entire body. Cilia are lost more rapidly from the dorsal surface posterior to the gill slits and mouth, and anterior to the caudal fin. The area of lower ciliary density ($\leqslant$1 cilium

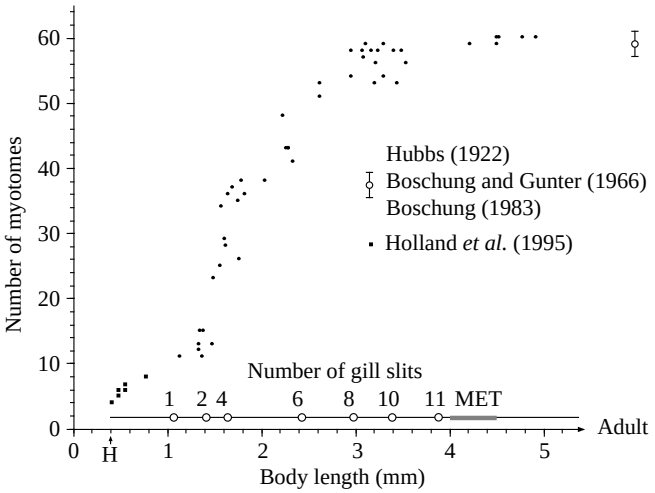

Fig. 1. The number of myotomes in the developing lancelet *Branchiostoma floridae versus* body length. Filled circles represent measurements using scanning electron microscopy, filled squares are taken from data in Holland *et al.* (1995). Mean and range (error bars) for adults (small open circle with error bars), 16–58 mm in total length, are taken from Hubbs (1922), Boschung and Gunter (1966) and Boschung (1983). The number of gill slits (large open circles) and the length at metamorphosis (MET) and at the time of hatching (H) are also shown.

per 100 μm^2) extends anteriorly and posteriorly until metamorphosis, at which point motile cilia are found only along the ventral sides of the snout, around the mouth and gill slits, and along the ventral body between the developing atrial folds (see Fig. 2). For other details regarding external morphology and other ciliated epidermal cells, see Stokes and Holland (1995*a*).

Because the motile cilia protrude from the centre of hexagonally shaped epidermal cells, they are uniformly distributed when they first appear on the body and on those body regions that retain higher densities of cilia. In all quadrate grids, the distribution was significantly different from an equal-area random distribution of cilia ($15 \leqslant G \leqslant 211$, $5 \leqslant N \leqslant 22$, $P > 0.005$) with calculated indices of dispersion (*I.D.*) close to 0 (mean ± S.D. *I.D.*=0.29±0.30, N=147), indicating a uniform, or regular, distribution pattern. As ciliary density decreased, in particular, along the dorsal surface and sides of the larval body, the distribution patterns showed an increased index of dispersion (closer to 1, which would indicate random dispersion) and/or distributions not significantly different from a Poisson distribution. For example, the dorsal surface of a 432 h larva had a mean *I.D.* of 0.971±0.23 (N=5), while the ventral surface had an *I.D.* of 0.18±0.054 (N=5) and the snout an *I.D.* of 0.213±0.12 (N=11).

Ciliary locomotion

The initial locomotory motions of lancelet larvae are powered exclusively by the body cilia, which move in metachronal waves. Prior to hatching, the neurula larvae rotate (in a clockwise direction when viewed from behind) in their fertilization envelopes, and this motion continues after hatching. A recently hatched larva describes a right-handed helix while swimming and shows a complex swimming path with its anterior end leading (Fig. 3A). This swimming path gradually straightens, and by 30 h after fertilization the larvae tend to move in relatively straight arcs. Larvae older than approximately 60 h show a slow dorsal arc while swimming (see Fig. 3A) or, if presented with a nearby surface, will glide along it with their right side against the substratum, showing a similar slow dorsal arc (if continued, the arc would form a circle

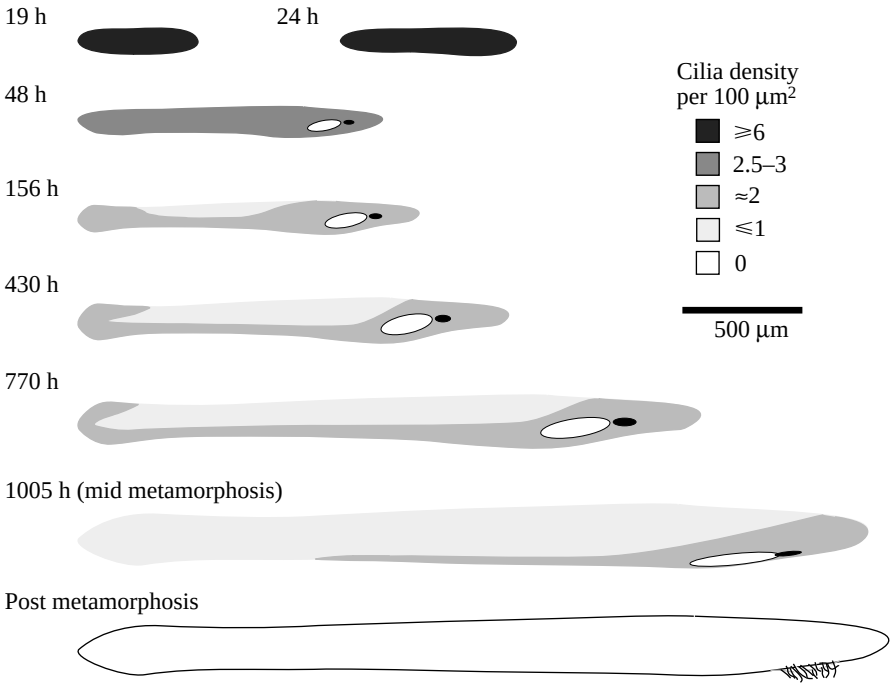

Fig. 2. Changes in the density and distribution of motile epidermal cilia during lancelet development. In all cases, anterior is to the right. The positions of the mouth (white oval) and preoral pit (dark oval) are also shown. The scale bar is 500 μm and $4 \leqslant N \leqslant 22$ samples. Specific cilia densities ±1 S.D. per 100 μm^2 for the developmental stages shown are: 19 h, 6.23±1.52; 24 h, 6.16±1.01; 48 h, 2.48±0.95; 156 h, 1.98±0.72; 430 h, 1.89±0.84; 770 h, 2.08±0.60; 1005 h, 2.02±1.01. For low-density (lightly shaded) areas: 156 h, 1.07±0.44; 430 h, 1.03±0.57; 770 h, 1.17±0.85; 1005 h, 0.18±0.01.

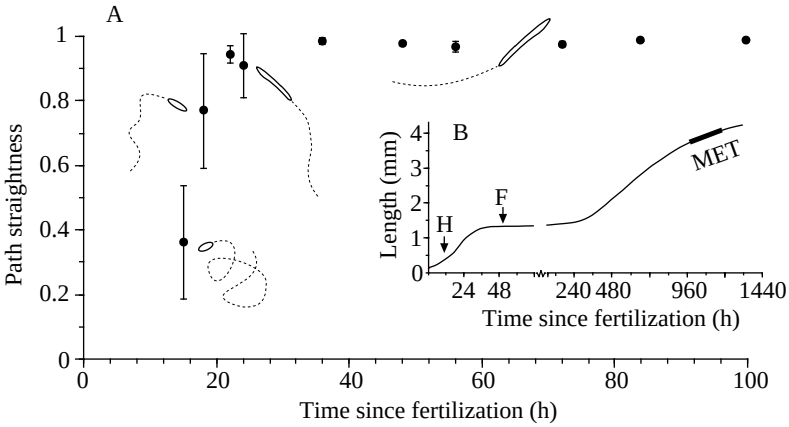

Fig. 3. (A) Changes in ciliary swimming path straightness during the first 100 h of lancelet development. In all cases, *N*=32 and error bars show ±1 S.D. Adjacent cartoons illustrate relevant path straightness values (see calculation in text) with dashed lines showing the path travelled by the larva. (B) Changes in body length *versus* time (h) after fertilization at a laboratory temperature of 22.5 °C. The time of hatching (H), first feeding (F) and metamorphosis (MET) are also indicated. Note the change in *x*-axis scale after 72 h.

of diameter approximately eight times the larval body length). This behaviour continues until metamorphosis; however, as indicated by Stokes and Holland (1995*b*), the predominant larval behaviour is to hover almost motionless in midwater.

The speed of ciliary swimming decreases over time since fertilization (Fig. 4). Recently hatched larvae swim at between approximately 0.6 and 1.0 mm s^{-1}. After approximately 60 h, swimming speed has decreased to less than 0.2 mm s^{-1}. The speed of ciliary gliding on the substratum decreases from approximately 0.18 mm s^{-1} at 100 h to 0.1 mm s^{-1} after approximately 1000 h, and gliding stops entirely at metamorphosis. The Reynolds numbers (calculated using larval body length) associated with these cilia-powered movements are between 0.02 and 0.3.

The velocity and flow pattern generated during ciliary locomotion vary a great deal during ontogeny. At all stages in development, fluid velocities were greatest (never exceeding approximately 1 mm s^{-1}) close to the lancelet body and diminished rapidly to unmeasurably low velocities within approximately 1 body length distance away from the individual (Figs 5, 6).

In 12 h larvae (Fig. 5A), flow speeds diminish more symmetrically about the body than at the later ages, although elevated fluid speeds extend slightly further in the larval wake. Streaklines indicate a circular flow pattern situated on both the dorsal and ventral sides of the body, and both patterns are centred slightly posterior to the body mid-section (in three dimensions, the flows are approximately toroidal). In 18 h larvae (Fig. 5B), the circular flows have increased in diameter and are centred closer to the anterior. Fluid speeds are greatest on the posterior half of the body.

Approximately 24 h after fertilization (Fig. 5C), the circular flows on the dorsal and ventral sides of the body are less noticeable because their diameter is now much greater than the body length of the larvae. The ventral flow centre has shifted towards the anterior end of the body, and maximal fluid speeds are found along the body mid-section and posterior half. With the development of the first gill slit at about this time and of the mouth approximately 24 h later, flow is directed posterio-ventrally from the larval anterior.

After the first 24 h and as the larvae increase in size, the flow field remains similar, with a few exceptions, until

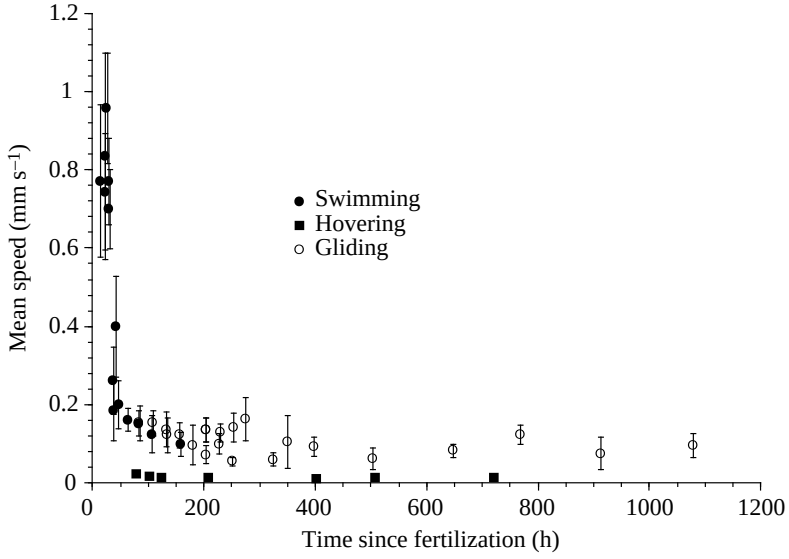

Fig. 4. Mean speeds attained by cilia-powered locomotion during the first 1200 h of lancelet development. In all cases, *N*=32 individuals and error bars show ±1 S.D. Different symbols indicate swimming (filled circles), hovering (filled squares) and gliding (open circles).

metamorphosis begins (at approximately 900 h). For example, at 670 h, flow is fastest along the ventral side of the body, and flow speeds are higher at the anterior in association with flow into the mouth and out of the nine gill slits and with the lack of dense dorsal cilia (Fig. 6A). Additionally, some flow is directed across the body from the ventral to the dorsal side in the caudal region starting near the anus. During further development, flow decreases along the dorsal surface and by 960 h (Fig. 6B, mid-metamorphosis) dorsal flow speeds are less than 0.1 mm s^{-1} over much of the body. The development of the atrium alters the fluid flow along the ventral side of the larvae. Flow is still rapid and directed anteriorly along the ventral surface behind the gill slits; however, because the atrium encloses some of the gill slits, flow is directed out of the atriopore as a small jet as well as out of the remaining uncovered gills.

The amount of water exiting the atriopore increases as metamorphosis continues and more of the gill slits are enclosed by the atrium. At the same time, flow ceases along the ventral surface as the atrium elongates and the remaining motile cilia disappear from the external epidermis. Ciliary powered locomotion and flow cease at metamorphosis, and in a

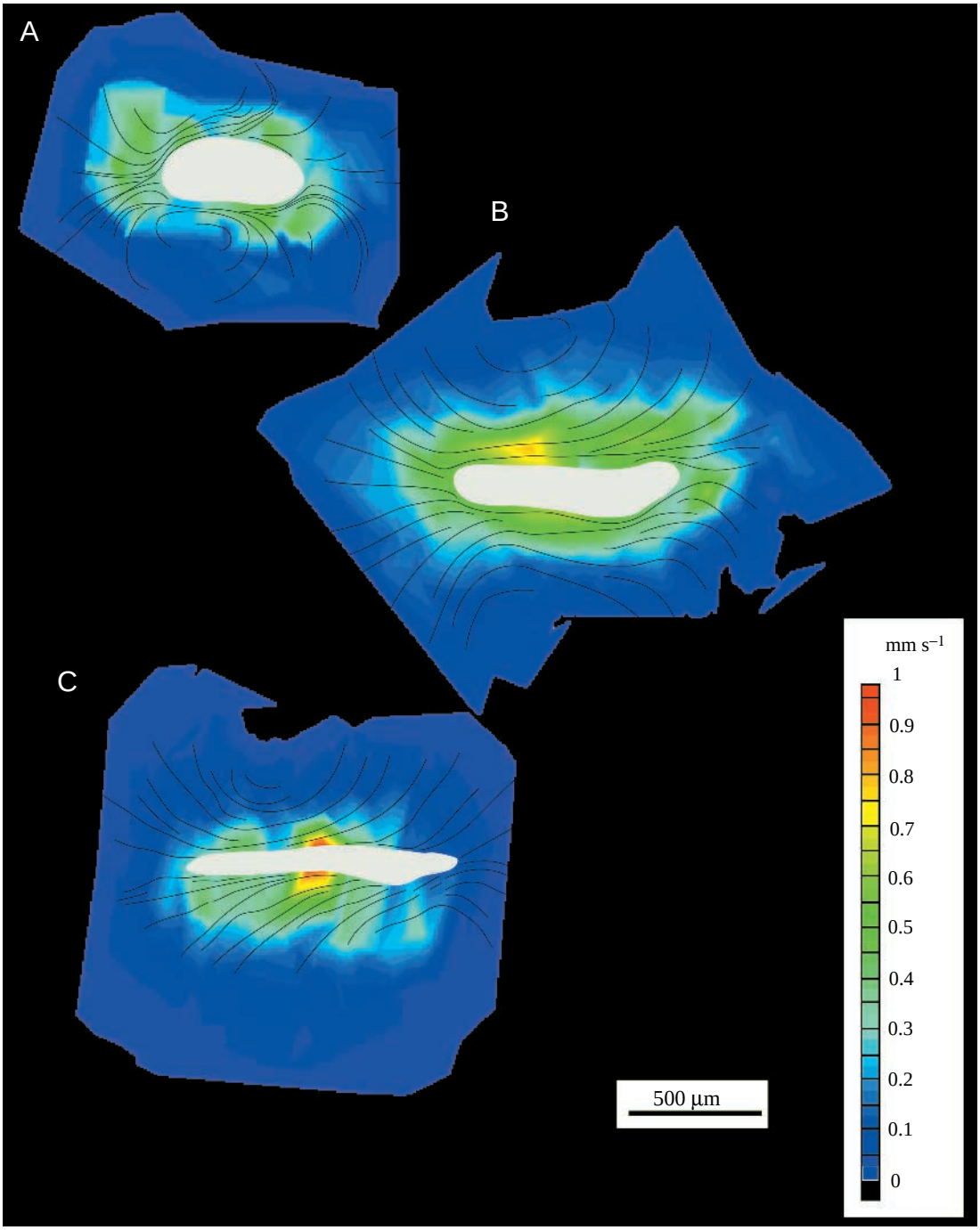

Fig. 5. Cilia-generated fluid flow around selected larval stages (lateral view); (A) 12 h larva; (B) 18 h larva; (C) 24 h larva. Streaklines show flow direction and the colour scale contouring indicates flow speed in the reference frame of the larva. In all cases, anterior is oriented towards the right, and all larvae are swimming from left to right. All images were produced as mosaics by superimposing particle traces from over 100 video frames for each subject. Scale bar, 500 μm.

stationary juvenile the only flow is associated with the feeding current into the mouth and out the atriopore (Fig. 6C).

Undulatory locomotion

Muscle-powered body motions first occur in larvae approximately 16 h after fertilization. After approximately 72 h, the first simple flexions have increased in complexity, frequency and duration such that the undulatory wave produced by the body and the resulting locomotion are nearly identical to those in the adult, although at a slower translational speed.

At 16 h, the initial muscle motions are slow (approximately 0.5 s duration) with flexions towards only one side of the body (Fig. 7). A flexion is equally likely to be to the left or to the right. The motions occur either singly, between long periods of ciliary swimming (seconds to minutes in length), or in a rapid sequence of two or three successive twitches with no preference as to the side of bending. By 18 h, the body no longer bends to one side only, but includes bends to one side followed by bends to the other side. However, the successive bends do not always follow in an alternating pattern (Fig. 7).

Approximately 20 h after fertilization, swimming larvae punctuate ciliary locomotion with longer bouts of muscular undulation lasting for as long as 90 s (Fig. 7). Most of the

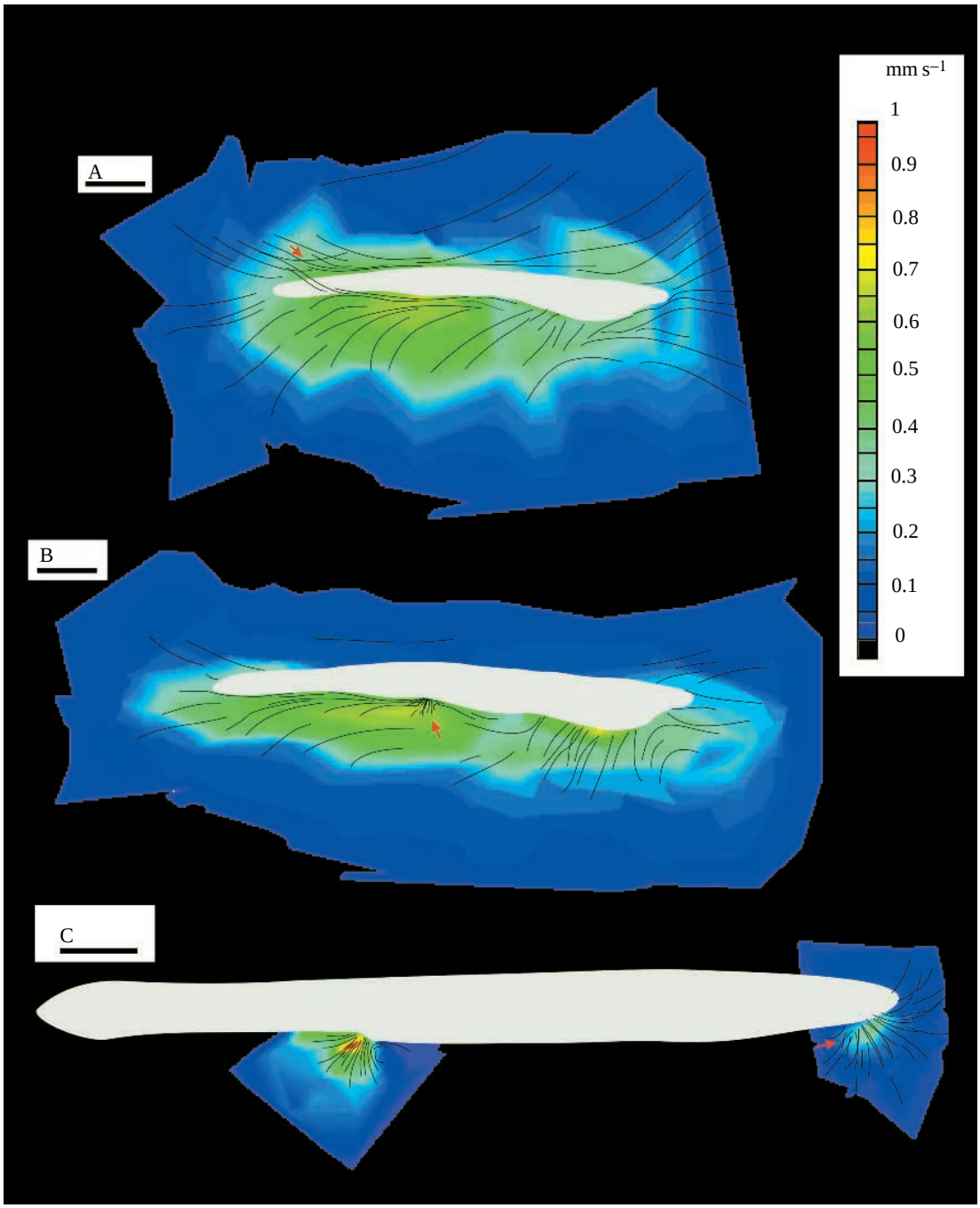

Fig. 6. Cilia-generated fluid flow surrounding 670 h (A), 960 h (B) and juvenile (post-metamorphic) (C) lancelets (lateral view). Imaging details are as in Fig. 5. Some ‘crossing’ of streaklines is indicated where fluid flow is directed out of the image focal plane, but is still visible (e.g. at red arrows). The juvenile lancelet is stationary, and streaklines and velocity contours indicate flow generated in the region of the mouth and atriopore by feeding activity. Scale bars, 500 µm.

muscular motion involves bending towards alternate sides of the body; however, groups of one-sided bends between short intervals (0.1 s) of ciliary swimming still occur. The bends produced by the body have a greater amplitude than do those of younger larvae and incorporate approximately 50 % of a sinusoidal wavelength. Over the next 8 h, the amplitude of the

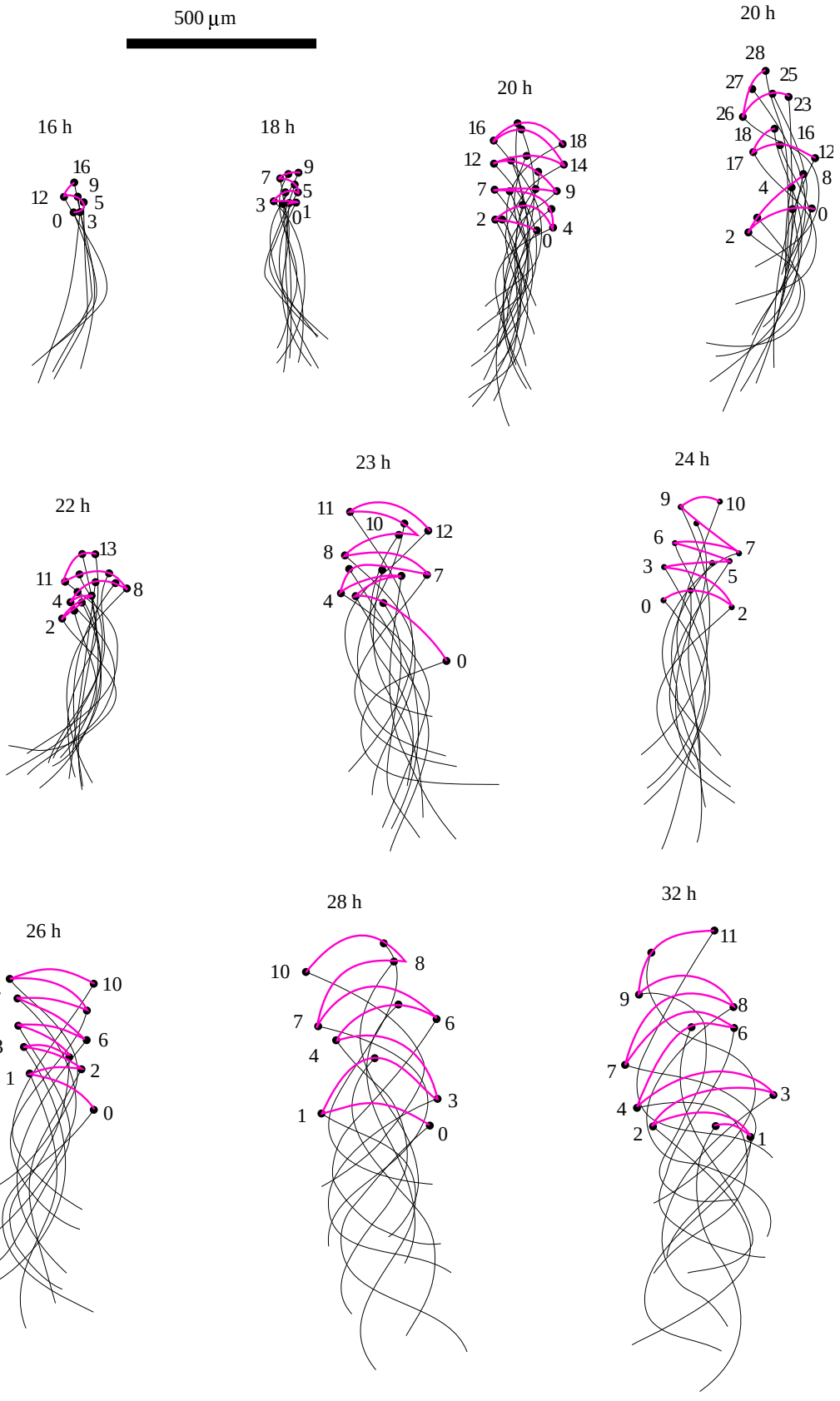

Fig. 7. Changes in body position during undulatory motion during the first 32 h post-fertilization as viewed from above. The fine lines trace the dorsal midline of the body and the anterior end is marked by a dot. In all cases, larvae move from the bottom towards the top of the figure. Scale bar, 500 µm. The red line traces the path of the anterior end during undulation. Numbers at the anterior end of body traces indicate the frame sequence number (video frames are 1/30 s apart, all sequences start at 0).

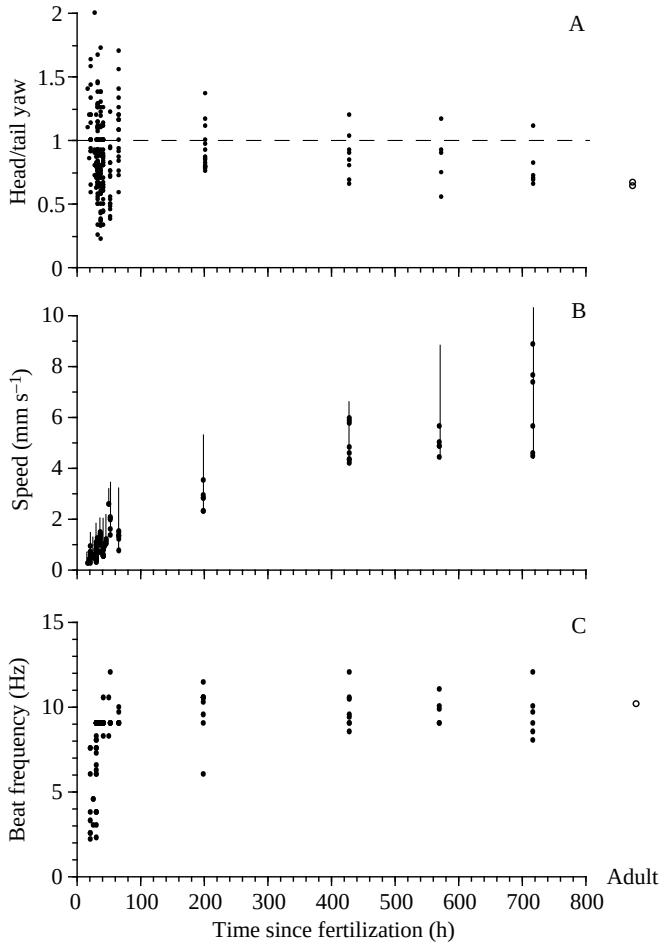

Fig. 8. Changes in undulatory swimming kinematics during the first 800 h of lancelet development. (A) Head/tail yaw, (B) swimming speed, (C) undulatory beat frequency. Open circles represent adult values for yaw and beat frequency taken from data in Webb (1973, 1976*a*). Adult swimming speeds are 30–60 cm s^{-1}. Each point is an average taken from a number of different observations ($1<N<25$) on the same individual. The maximum range of swimming speed is shown by the vertical line (minimum swimming speed was 0 cm s^{-1}).

undulatory waves increases from a small fraction to approximately 17 % of the body length, the regularity of the undulatory beating increases, and the undulatory wave on the body begins to incorporate a full wavelength. By 28 h, the larvae can generate a full undulatory wave that propagates down the body for propulsion.

During undulatory swimming, the head shows considerable yaw. Swimming larvae can move their anterior ends as much as 90 ° from the centre line of motion (although 50 ° is more typical). The relative amount of head/tail yaw is shown in Fig. 8A. Over the first 72 h of development, there is large variation in head/tail yaw, with either the head or tail displaced farther from the centre line of motion during undulation. This variation decreases over time and, by metamorphosis the degree of head/tail yaw is similar to that seen in the adult (approximately 0.7).

Over the first 24 h, the body undulations appear to generate little thrust for the swimming larvae. The undulating larvae progress no faster than by cilia-powered swimming alone (Fig. 8B). Undulatory swimming speeds increase from less than 1 mm s^{-1} to 2 mm s^{-1} by 48 h after fertilization and coincide with the development of a fully propagating wave. Swimming speed continues to increase during development and larvae are capable of short bursts at speeds as fast as 10 mm s^{-1} by the time of metamorphosis. The frequency of undulatory beating (i.e. the frequency of complete wave propagation) increases rapidly during early development (Fig. 8C). The initial undulatory twitches and bends occur at a frequency of approximately 2–3 Hz but increase in frequency until, after 48 h, the beat frequency reaches a plateau at approximately 10 Hz (equivalent to the typical adult swimming beat frequency; Webb, 1976*a*).

High-speed undulation

In addition to ciliary swimming, hovering and undulatory locomotion, lancelet larvae, after approximately 60 h after fertilization, are also capable of extremely rapid body movements (Fig. 9B–K). From high-speed video analysis (at either 500 or 1000 frames s^{-1}), it is apparent that these muscular movements are somewhat similar to regular undulatory swimming motions, but occur at a much higher beat frequency, are irregular in pattern and are less coordinated than normal swimming (Fig. 9A). Such movements occasionally occur spontaneously when larvae are hovering in mid-water, but they are most common when larvae are gliding on a surface. In these cases, if the larvae are oriented left-side down (such that their mouth is against the substratum), they remain motionless for a short period (usually less than 60 s) and then rapidly twitch from the bottom using tight contractions of the body forming a ‘C’ or ‘S’ shape (Fig. 9B–K). Afterwards, they settle back to the substratum, or sometimes swim away using a regular undulatory beat. If they land left-side down following the violent twitching, the cycle repeats itself. If they land right-side down (mouth upwards), they glide away using their cilia.

During this rapid ‘twitch-flip’ behaviour, the larvae are capable of producing full flexure to one side of the body in approximately 1/100 s (0.011±0.004 s; mean ± S.D., N=26) and although it is difficult to measure a true beat frequency, because the undulation is so irregular, a full cycle of beating can be estimated to be 5–10 times faster than during regular swimming. Additionally, these rapid movements usually do not result in much net forward motion. The violent flipping often results in the larva progressing sideways (e.g. Fig. 9B) or backwards (e.g. Fig. 9I) or results in no overall movement (e.g. Fig. 9J).

An escape reaction performed by a post-metamorphic juvenile (12 mm in length) is shown in Fig. 9L. The lancelet was touched on the caudal region with a sharp wire at time 0 and the individual reacted using a series of rapid undulations followed by reverse swimming (tail first) away from the stimulus. These muscular motions appear similar to the ‘twitch-flip’ of larvae, although they are slower. Post-

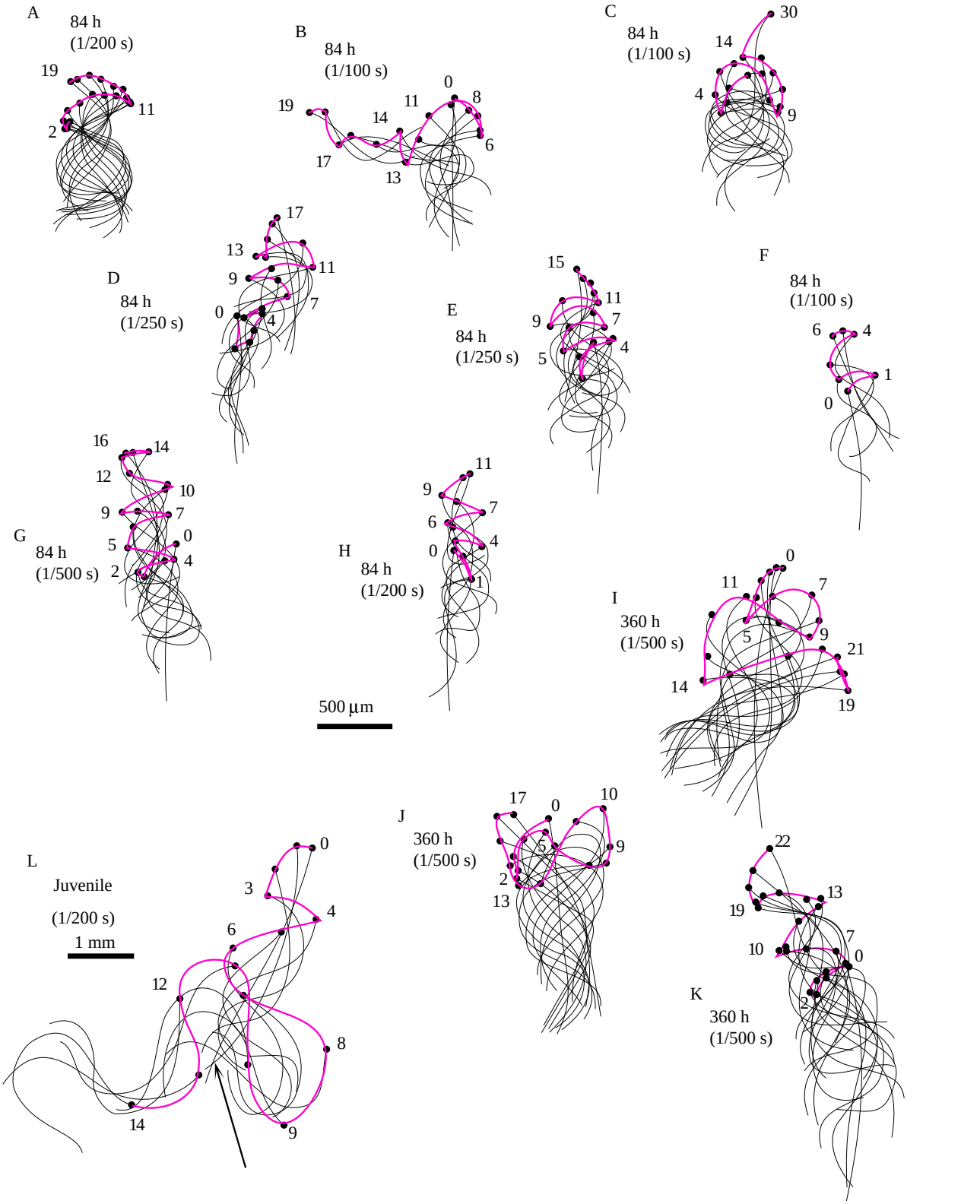

Fig. 9. Changes in body position during undulatory swimming taken from high-speed video sequences (500 and 1000 frames s^{-1}) of larvae at either 84 h (A–H) or 360 h (I–K) post-fertilization and of a juvenile (L). Fine lines represent the position of the dorsal midline (viewed from above), and the solid dot indicates the anterior end. In all cases, the lancelets are initially positioned with their anterior end pointing to the top of the figure. The red line traces the path of the anterior end during undulation. The time interval between successive body traces is indicated in parentheses and the numbers at the anterior end indicate the frame numbers (all sequences start at 0). (A) Normal swimming; (B–K) examples of the rapid 'twitch-flip' behaviour (see text for further details). (L) The escape reaction of a juvenile after being touched by a sharp wire in the position shown by the arrow. Scale bars, A–K, 500 µm; L, 1 mm.

metamorphic lancelets apparently lack the high-speed behaviour shown by the larvae. Additionally, swimming caudal-end first is often seen in post-metamorphic lancelets, but was not observed in the larvae except during 'twitch-flip' behaviour.

Comparison of ciliary and undulatory flow fields

A reconstruction of fluid motion around 24 h larvae swimming using either ciliary or undulatory movements reveals large differences in the flow patterns (Figs 10, 11). During a 0.1 s interval, the fluid motion around a larva swimming using only its cilia is constrained to an envelope of fluid close to the body, and flow speeds are generally less than 1 mm s^{-1} and directed towards the posterior. Fluid motion was negligible a distance greater than approximately 250 µm from the larva.

Fluid motion around the undulating larva over the same 0.1 s time interval was very different. To approximate the flow field, the decay in particle motion with respect to distance (x) from the undulating body was measured. This relationship had an exponential form, $F(x)=0.1776e^{-11.832x}$ ($r^2=0.81$ $N=32$, $P>0.05$) and was used to calculate the particle motion (as a proxy for the actual flow field) resulting from one complete beat cycle. Fluid particles tended to oscillate normal to the long

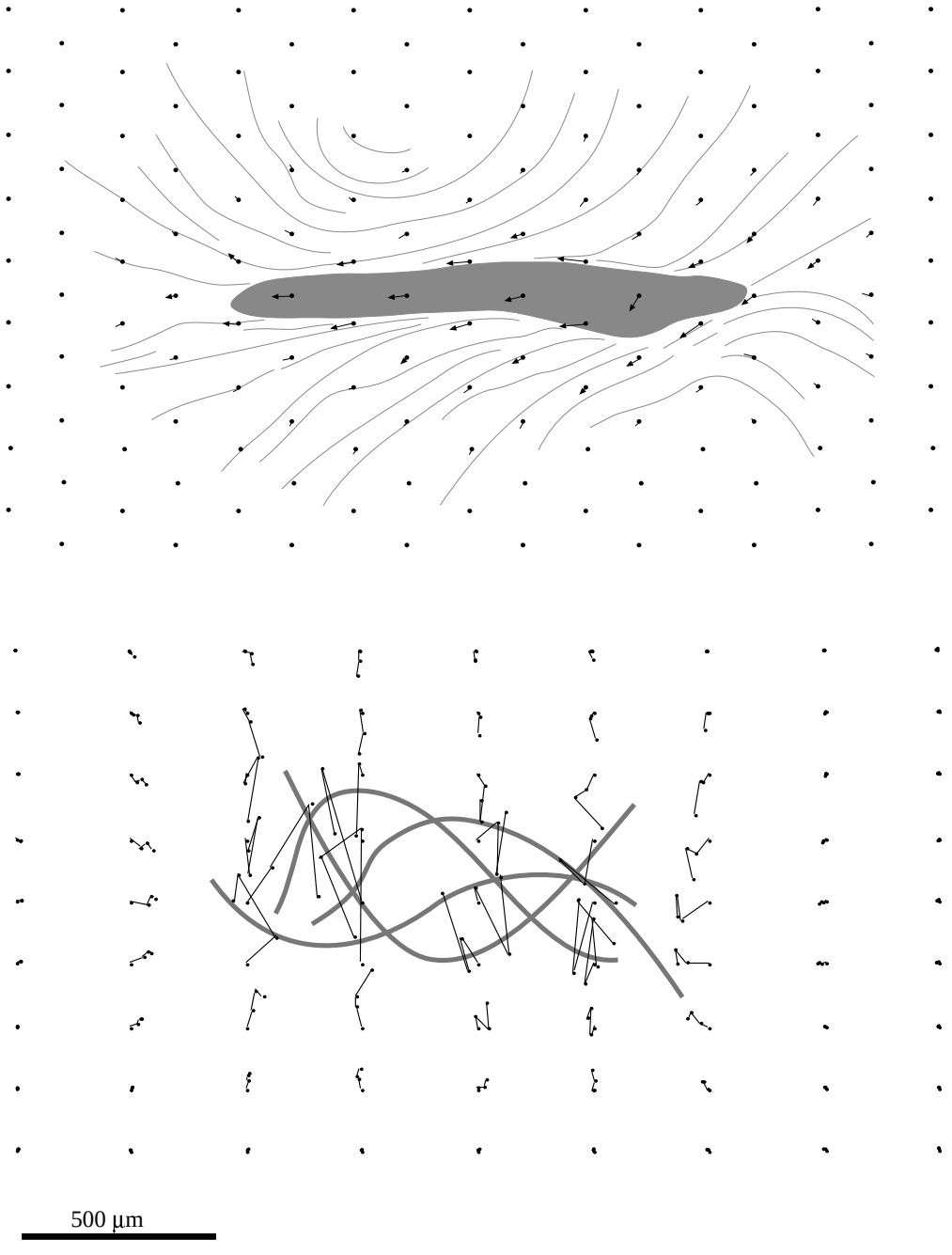

Fig. 10. Comparison of the flow field and particle trajectories over a 0.1 s interval for a ciliating (upper) and undulating (lower) 24 h larvae. Both larvae are oriented with anterior to the right; only the dorsal midline position is shown for the undulating larva. Individual particles were arranged in a regular array (162 or 81 points) at time zero. For the ciliating larva, vector arrows represent the direction and magnitude of particle net displacement in the 0.1 s interval. For the undulating larva, particles oscillate with the body movements, and vector arrowheads have been omitted for clarity. Scale bar, 500 µm.

axis of the undulating larva, with maximum oscillations near the sections of body that undergo the largest changes in amplitude during the beat cycle and in the fluid closest to the body (Figs 10, 11). Particle velocities were as high as 3 mm s^{-1} in the region of fluid influenced by the posterior third of the larval body. Particle velocity did not diminish to zero until more than 700 µm from the undulating body.

Energy expenditure during ciliary and undulatory swimming

The estimates for the energy dissipated during ciliary locomotion fall into three different groups (Fig. 12). The Keller and Wu (1977) model estimated that the power outside of the ciliary envelope (beyond the tips of the cilia) for a free-swimming larva ranged from approximately 10^{-12} W in a recently hatched larva to approximately 10^{-14} W in a 1000 h larva. Alternatively, for an inert larva (i.e. a sedimenting larva without beating cilia; Keller and Wu, 1977) and to overcome the viscous drag of a prolate spheroid (Emlet, 1994), the power requirements ranged from 10^{-11} W to approximately 10^{-13} W for recently hatched and 1000 h larvae, respectively.

Estimates of the energy dissipated within the ciliary sublayer (in the zone between the epidermal surface and the cilia tips) ranged between 10^{-9} W for recently hatched larvae and approximately 10^{-11} W for 1000 h larvae. The Keller and Wu (1977) model showed an increase in power from approximately 10^{-11} W to 10^{-10} W during the first 75 h before a reduction to approximately 7×10^{-10} W for larvae older than approximately 150 h. In contrast, the Roberts (1981) model showed a decrease in power from approximately 10^{-9} W to approximately 7×10^{-10} W over the same period. In all the models examined, ciliary power tended to remain constant after approximately 200 h of development.

In estimating the energy expenditure during undulatory swimming, both the Roberts (1981) and Azuma (1992) models gave similar results (Fig. 13). Undulatory power increased from approximately 10^{-12} W (model of Roberts, 1981) and

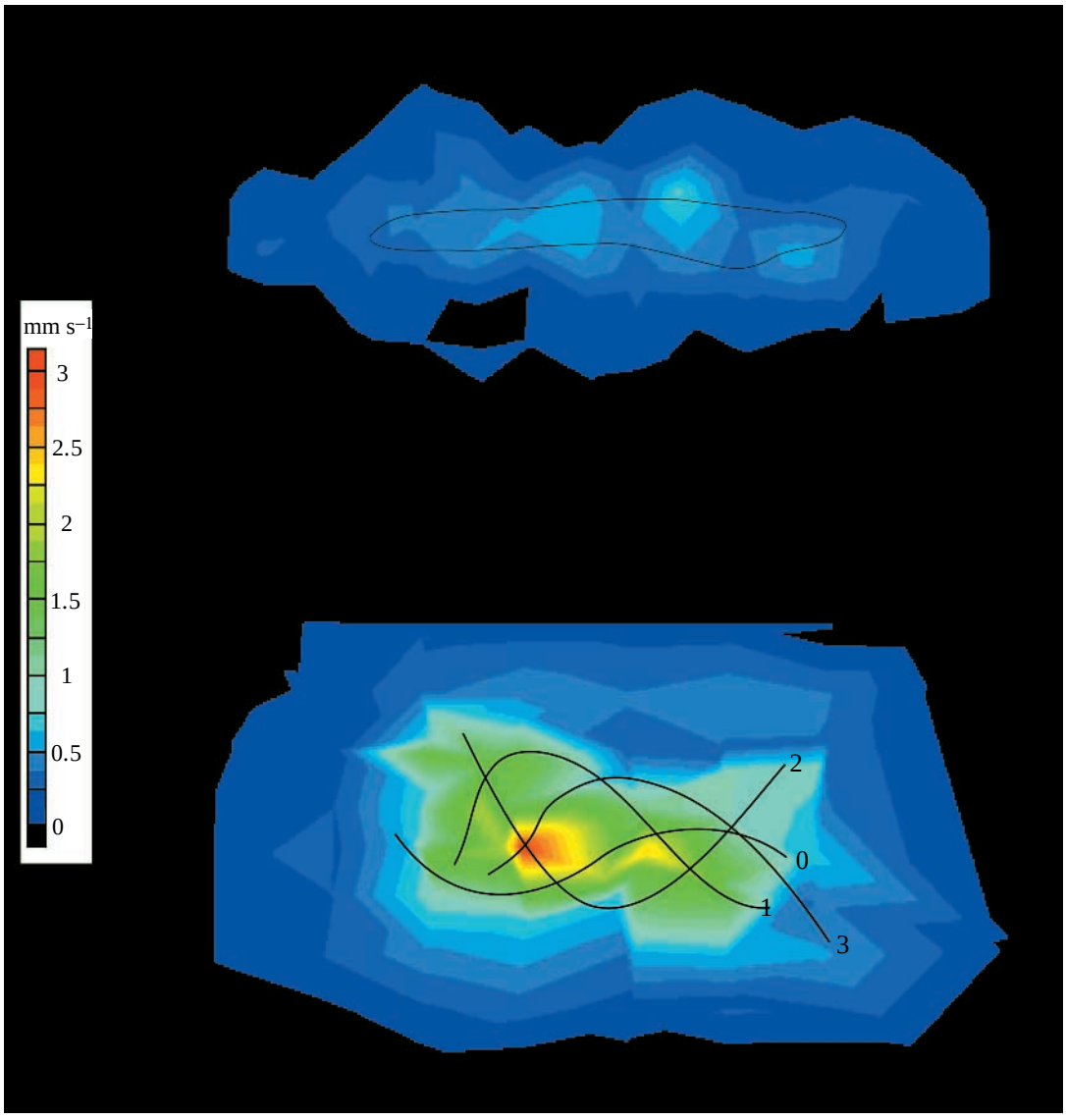

Fig. 11. Contours of fluid speeds around a ciliating (upper) and undulating (lower) 24 h larva generated in a 0.1 s interval. Speeds were calculated from the particle movement patterns shown in Fig. 10. Scale bar, 500 µm. For the undulating larva, numbers at the anterior end of the body (the dorsal midline is shown as a line) indicate successive frames, 1/30 s apart.

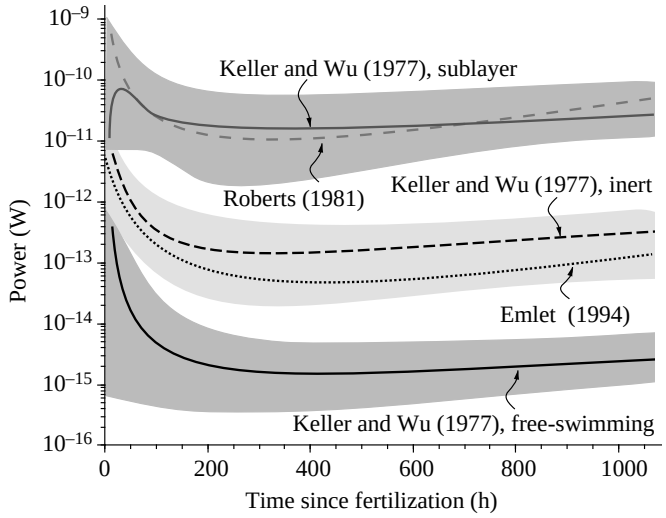

Fig. 12. Energy expenditure for lancelet ciliary swimming during the first 1000 h post-fertilization. Curves were fitted by eye to model data, shaded areas indicate the range of model values for estimates incorporating maximum/minimum and average swimming speeds (from Fig. 4). Models give the energy expended by free-swimming larvae (Keller and Wu, 1977) and by inert and/or sedimenting larvae (Keller and Wu, 1977; Emlet, 1994) and the energy expended within the ciliary sublayer (Keller and Wu, 1977; Roberts, 1981).

10^{-11} W (model of Azuma, 1992) in recently hatched larvae, to approximately 10^{-9} W at 50 h after fertilization. Energy expenditure after this period increased more gradually to approximately 10^{-8} W and 10^{-6} W for the Roberts (1981) and Azuma (1992) models, respectively. In both cases, model estimates were greatest using the Wu (1977) calculation of the viscous drag coefficient. The Gray and Hancock (1955) and Cox (1970) methods of estimating the viscous drag coefficient yielded similar results.

Discussion

Remarks on fluid flow

The small size and slow swimming speeds of the lancelets in this study constrain fluid flow to a Reynolds number (*Re*) regime of $Re<20$ and predominantly to $Re<1$. For ciliating larvae, using body length as the characteristic length in the calculation, *Re* ranged from approximately 0.01 to 0.2. At these low *Re* values, flow is dominated by viscosity, and inertial effects can be neglected, greatly simplifying mathematical description (Vogel, 1981). In undulating, pre-metamorphic lancelets, *Re* ranged from approximately 0.6 to a maximum of approximately 20. These *Re* values range from the low into the intermediate *Re* realm ($1<Re<1000$). The exact lower boundaries of the intermediate realm have been estimated subjectively to be between 1 and 10 by various researchers (e.g. Jordan, 1992). In this flow regime, neither viscous nor inertial forces can be neglected, complicating mathematical estimates of fluid motion. Despite this, Jordan (1992) showed that, after initial accelerations, a viscous model provides a good approximation of fluid forces under these conditions. In the present study, energy expenditure was estimated from models that neglect inertial forces, although, for those few calculations that did include motion in the intermediate *Re* realm, kinematic measurements were made and applied to periods of constant swimming speed.

At low *Re*, the presence of a solid boundary near a small moving body can greatly affect the dynamics of fluid motion (the 'wall effect'; Roberts, 1981; Vogel, 1981; Chia *et al.* 1984). The presence of any walls in this flow regime can increase the drag experienced by a swimming organism (Winet, 1973), so all measurements of particle and larval velocity must be considered to represent a minimum. However, because swimming larvae were generally observed in the centre of the observation dish, away from the bottom and walls, wall effects were likely to be minimized, and because the same vessel was used for all observations, the effects were constant. With the exception of the gliding larvae, for which fluid flow altered by the presence of a solid boundary would be the natural situation, the experimental conditions were such that wall effects as estimated by Vogel (1981) were probably very small, if not negligible.

The reconstruction of fluid motion around an undulating larva (Figs 10, 11) is an approximation of the actual hydrodynamic flow. This is a simple one-dimensional solution (incorporating exponential decay along an axis normal to the moving body) to what is truly a multi-dimensional problem which includes a three-dimensional flow field as well as a time component. For the purposes of the present investigation, it simply shows the area of influence of the undulatory motion and indicates that higher fluid speeds occur compared with those during ciliary swimming.

Ciliation

Ciliated larvae are not unknown among vertebrates. The larvae of the primitive fishes *Protopterus aethiopicus* (Budgett, 1901; Greenwood, 1958), *Neoceratodus forsteri* (Kemp, 1996), *Polyodon spathula* (Bems and Grade, 1992), *Lepisosteus platyrhincus* (Song and Northcutt, 1991) and some amphibians (Steiner, 1939) retain epidermal ciliation for a short time during their early development. These ciliated embryos are often considered to represent a phylogenetic recapitulation and may help to move water over the gills, and keep the epidermis free of settled particles (Kemp, 1996), rather than having a specific locomotive adaptation. In contrast, lancelets use their epidermal cilia extensively for locomotion (swimming, hovering, or gliding) until metamorphosis in addition to other possible functions such as improving gas exchange.

Ciliating lancelet larvae swim at similar speeds to other like-sized ciliated organisms. Most comparable speed measurements have been made on protozoa (e.g. Machemer, 1972; Keller and Wu, 1977; Sleigh and Blake, 1977; Sleigh, 1989) and a few species of planktonic invertebrate larvae (Chia *et al.* 1984; Emlet, 1990, 1994), and speeds of approximately 1 mm s^{-1} are typical (Sleigh and Blake, 1977). Recently

hatched lancelet larvae swim using a helical pathway that has caused some speculation regarding its origin and significance (e.g. Knight-Jones, 1954; Insom *et al.* 1995). Spiral swimming and rotation are probably a result of the beating of cilia associated with the mouth and gill slits, an asymmetry in larval shape, and slight regional differences in the beat frequency and direction of the ciliary metachronal waves in a manner similar to that seen in the swimming of *Paramecium* sp. and other microorganisms (Naef, 1926; Naitoh and Sugino, 1984).

Reduction in the density of cilia is correlated with changes in swimming speed and in the pattern of fluid flow along the body. For example, flow is almost negligible along the dorsal surface of the 960 h larvae (Fig. 6B), which correlates with the progressive loss of epidermal cilia along that part of the body (Fig. 2). After the opening of the gill slits, thrust is directed posterio-ventrally away from the anterior of the body. Later in development (e.g. at 670 h), some fluid is directed dorsally in the region of the caudal fin and anus. Both of these forces tend to rotate the larva dorsally, at its anterior end, around its centre of mass. This may explain the backwards-arcing pathway seen in swimming and gliding larvae a few days after fertilization as well as the tilted body posture seen during hovering behaviour (Stokes and Holland, 1995*b*).

In addition to the ciliated epidermal cells considered here, there are other ciliated regions on the lancelet. In the region of the mouth, gill slits, preoral pit, and possibly the ciliary tuft (Stokes and Holland, 1995*a*) and anus, flow is visibly altered around the larva. However, although thrust is produced by the generation of feeding currents through the motion of water into the mouth and out of the gills slits (and later the atriopore), this seems to be a relatively unimportant source of thrust for ciliating larvae. Larvae with their anterior end excised behind the gill slits and abnormal larvae lacking a mouth opening move through the water at approximately the same speed as normal larvae (data not shown). Additionally, observations of fluid flow around the larvae suggest that it is the epidermal cilia of the body that provide the majority of thrust for forward motion, and the loss of these epidermal cilia during development leads to slower swimming and gliding speeds.

Undulation

Despite detailed treatments of undulatory swimming (e.g. Lighthill, 1975), the early ontogeny of larval vertebrate swimming kinematics remains relatively unstudied (see reviews in Blaxter, 1969; Hunter, 1981). Available studies have tended to concentrate on commercially important fish species such as anchovy and herring, which have early developmental stages at least an order of magnitude larger than amphioxus. Also, these studies tend to focus on questions relating swimming performance to larval energetics rather than on the descriptive ontogeny of early larval movements (Blaxter, 1969; Weihs, 1979; Hunter, 1981; Batty *et al.* 1991). A comprehensive study of the ontogeny of locomotor kinematics in the cyprinid *Danio rerio* (Fuiman and Webb, 1988) only considered changes in later stages, after undulation had fully developed. The early locomotor responses to mechanical stimulation along with coincident changes in the spinal cord neurones in the primitive Australian lungfish *Neoceratodus forsteri* (Whiting *et al.* 1993) have been examined, and the neuromuscular development of the

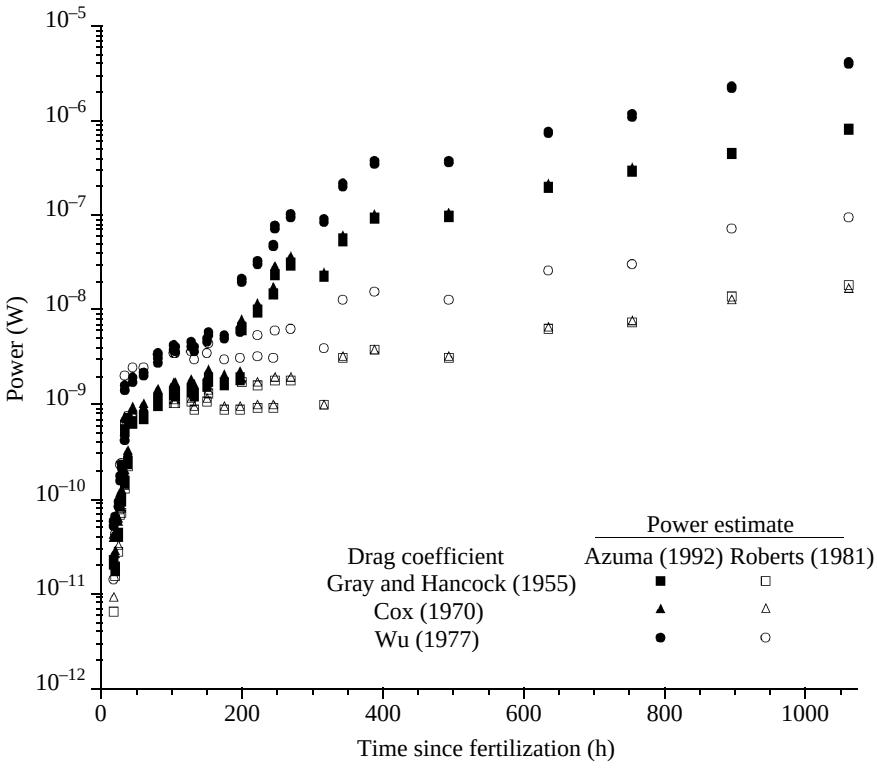

Fig. 13. Energy expenditure for lancelet undulatory swimming during the first 1000 h post-fertilization. Power estimates were calculated using low-Reynolds-number undulatory models from Roberts (1981) (open symbols) and Azuma (1992) (filled symbols). Each model was calculated using estimates of the viscous drag coefficient from equations given by Gray and Hancock (1955), Cox (1970) and Wu (1977).

amphibian *Xenopus laevis* has also received extensive study (e.g. van Mier *et al.* 1989; Sillar and Roberts, 1993; Roberts and Tunstall, 1994). However, both lungfish embryos (5 mm long) and those of *Xenopus laevis* (>3 mm long) are much larger than larval amphioxus when muscle movements first occur, and a complete kinematic treatment of developing locomotion is still lacking. Some changes in the tailbeat frequency and underlying motoneurone activity in larval angelfish *Pterophyllum scalare* have been reported (Yoshida *et al.* 1996). However, these larvae are also much larger than the lancelet (4 mm long), and they are unusual in that they remain attached to the substratum, *via* cement glands in their heads, for 4–5 days after hatching.

Although kinematic data for microscopic animals moving using muscular undulation are scarce, the undulatory beat frequency and changes in swimming speeds in larval lancelets are similar to observations that have been made on similar-sized Mastigophora, nematodes, small polychaetes (Holwill, 1974, 1977; Azuma, 1992) and ascidian tadpoles (Bone, 1992). Tailbeat frequencies as high as 50 Hz have been observed in larval anchovy and mackerel (Hunter, 1981), and for fish in general tailbeat tends to scale inversely with body length. The lancelet body shows a large anterior yaw while swimming, sometimes displacing itself 90° from the axis of motion. Ascidian tadpoles (Bone, 1992) similarly show a wide yaw while swimming. In larger animals operating at higher *Re*, more efficient and faster swimmers minimize head yaw to decrease drag and increase propeller efficiency (Webb, 1993; Wardle *et al.* 1995). Minimizing drag in this manner is not as important in the relatively low *Re* realm experienced by the swimming lancelet larvae.

It was recognized by Bone (1958) that the development of muscular movement in lancelets occurred very early as opposed to Garstang's (1928) beliefs. Bone (1958) observed early flexions at approximately 27 h post-fertilization, and more rapid body undulations at approximately 90 h. These observations were made on *B. lanceolatum*, which apparently develop at a slower rate than *B. floridae* (Stokes and Holland, 1995*a*). The first muscle movements in *B. floridae* occurred approximately 16 h after fertilization and these movements were essentially fully developed after approximately 30 h.

Coghill (1908), examining the embryo of the amphibian *Triton torsus*, saw the first muscular movements as flexure near the embryonic head. As the embryo aged, the reaction progressed caudally until the entire trunk was involved, gradually developing into S-shaped bends. This apparently reflected the migration of the cranial nerve roots caudally during development. The development of swimming in *Xenopus laevis* shows a progression from irregular contractions on alternating sides of the body to fully developed undulation coincident with the caudal progression of primary motoneurones in the spinal cord and the development of a critical number of neural connections in the central pattern generator (van Mier *et al.* 1989; Roberts and Tunstall, 1994). Initial flexures in *Neoceratodus forsteri* embryos were also near the anterior end (Whiting *et al.* 1993). A similar progression of flexure caudad was not seen in the larval lancelet in the present study. The first motions appeared at the level of the mid-body, and the amplitude of the flexure and the wavelength of undulation increased during ontogeny until a fully developed wave could be propagated down the body by approximately 30 h post-hatching.

When the first body flexures occur, lancelet larvae have approximately six or seven myotomes and are approximately 600 μm long. For comparison, the first spontaneous muscle contractions occur in the zebrafish *Danio rerio* embryo at 18 h, when it has approximately 18 somites and is approximately 2 mm long (Kimmel, 1993), and, in the amphibian *Xenopus laevis*, the first muscle flexures occur around stage 26 (approximately 17 somites) and approximately 3 mm long (van Mier *et al.* 1989; Sillar and Roberts, 1993). By 30 h post-fertilization, and full undulatory wave production, the lancelet larvae have 11 or 12 myotomes and are approximately 1200 μm long (Fig. 3B). In addition to requiring the development of the correct neural and muscular systems to generate (and then propagate) a complete sinusoidal wave, it may be physically impossible to bend the larval body through more than 1 degree of flexure (i.e. half a sinusoidal wavelength) until a minimum number of myotomes have formed. Until that time, muscle contraction against the notochord, which acts as a flexible strut, may only produce bending with 1 degree of flexure centred midbody. Blight (1976, 1977) distinguished between passive wave propagation down the body dependent upon the material properties of the body (in particular the notochord) and the dynamic propagation of a wave down the body due to the sequential contraction of myotomes. For effective locomotion, it is the propagation of the waves that is important, not the nature of the bend formation. In lancelets, the first body motions do flex the body, although this movement is not effective for locomotion until the bend(s) can travel down the body. This is essential in the low *Re* realm of the larvae because of temporal asymmetries in fluid flow (Vogel, 1981).

Even when undulatory swimming behaviour has developed completely, it is not known to what degree wave propagation is a result of differential stiffness in the amphioxus notochord or a result of sequential nervous stimulation of muscle myotomes. The notochord of amphioxus is a complex and highly specialized hydrostatic organ containing fluid-filled vacuoles, paramyosin filaments, ventral root connections to the dorsal nerve cord and other specialized cells (reviewed by Flood, 1975). It has been suggested by Webb (1973) that forward and reverse swimming in the adult is associated with stiffening of either the anterior or posterior end of the notochord, respectively. If this is the case, the material properties of the notochord undoubtedly have an important role in undulatory wave propagation and may function as a dynamic strut under neuromuscular control (Guthrie and Banks, 1970; Guthrie, 1967, 1975). The behavioural data in the present paper should be correlated with the detailed cytological development of the larval nervous system and notochord during the crucial first 30 h after fertilization established using the reconstructive techniques of Lacalli *et al.* (1994) and Lacalli (1996).

The undulatory swimming of a larva, once fully developed,

is essentially the same as in the adult, and shows a similar wave form, beat frequency and degree of yaw (Webb, 1973, 1976*a*). Adults can swim faster than larvae owing to their larger size and because they are moving in a medium that is no longer governed strictly by viscous forces, but also by inertia.

High-speed undulation

The high-speed undulation of amphioxus larvae was first observed by van Wijhe (1927) and also by Wickstead (1967), who noted that the larvae occasionally flipped off the bottom if lying on their side, in order to begin feeding. With the aid of high-speed video analysis (Fig. 9), it can be seen that this behaviour takes the form of an extremely rapid burst of body undulations lacking the coordination of normal swimming. This motion is different from the C- or S-start of a rapidly accelerating fish (Webb, 1993) or the escape response seen in a juvenile lancelet. Body flexure occurs faster than in the juvenile escape response and there is no controlled direction of travel during the violent twitching, unlike in a fish C- or S-start. Despite a lack of coordination, this high-speed undulation response of amphioxus larvae does result in reorientation of the body for feeding if lying on a substratum and may also function as an escape response for evading capture by planktonic predators.

The ability of the lancelet to swim rapidly both forwards and backwards was believed by Webb (1973, 1976*a*) to be a facility acquired after metamorphosis. Reverse swimming was not observed in the larvae of *B. floridae* in this study; however, their small size might have precluded this observation since it was sometimes difficult to discern the anterior from the posterior end during rapid undulation. Undulatory motions in the reverse direction were seen in pre-metamorphic larvae during the high-speed undulation behaviour (Fig. 9I), so backward movement might not be exclusively an adult attribute.

Power

The estimates of energy expenditure during locomotion by the ciliating larvae are similar to the few measurements available for other organisms and correlate well with direct estimates of the force exerted by hovering lancelet larvae (Stokes and Holland, 1995*b*). Within the cilia sublayer (the fluid layer surrounding the larvae with a thickness equal to the length of the beating cilia), the power expended by *Paramecium* sp., swimming at 2.5 mm s^{-1}, has been estimated as 6.7×10^{-11} W (Keller and Wu, 1977). The estimated power output in the lancelet ranged from approximately 10^{-9} to 10^{-11} W depending upon the age of the larvae and the model used. The Keller and Wu (1977) model produced a much lower estimate of the energy expenditure during the first 50 h of development than did the Roberts model (1981). This discrepancy is due to the manner in which power is estimated. The Keller and Wu (1977) sublayer model estimates power by making an integrated estimate of the total power expended by each cilium over the entire surface area of the organism. The total number of cilia on the lancelet epidermis first increases during growth and then decreases as the density of cilia begins to decline as larval size increases. The Roberts (1981) estimate of power depends upon larval ciliary swimming speed, which is greatest during this period. However, after approximately 100 h of development, both estimates yield very similar results despite their different approaches, and a power of 10^{-10} to 10^{-11} W may be a reasonable estimate of ciliary power production within the sublayer.

All other estimates of energy expenditure utilized swimming speed as a model parameter and thus show maximum power occurring during the first 100 h post-fertilization when ciliary swimming speeds were greatest. The Keller and Wu (1977) free-swimming model estimated that approximately 2–4 orders of magnitude more energy is expended within the sublayer than outside it. For recently hatched larvae, energy expenditure was approximately 10^{-12} W, which compares favourably with the 3×10^{-12} W estimated for *Paramecium* sp. (Keller and Wu, 1977). The radical difference in energy expenditure within the sublayer compared with outside it is due to the exponential decay of flow speeds away from a propeller (in this case the cilia, approximately 10 μm long) (Roberts, 1981; Blake and Sleigh, 1974). Power output is greatest within the sublayer in which the water is viscously entrained next to the cilia, and energy must be expended in accelerating and decelerating this fluid during each ciliary beating cycle. For consideration of total larval energetics, the energy expended outside the ciliary sublayer might be considered to be negligible. It should also be noted that these are estimates of minimum locomotory power and constitute only that portion of the total energy expended to modify the fluid flow during locomotion but do not include the energy expended by the individual for other processes (i.e. growth and differentiation, basal metabolism, heat production).

The efficacy of the Keller and Wu (1977) porous prolate model is illustrated by a comparison between the results of the energy expended in fluid flow around an inert larva (i.e. sedimenting at swimming speed *via* gravity) and the estimate by Emlet (1994) for a passive body moving through a fluid at the same swimming speed. Both estimates give approximately 10^{-12} W depending on the speed of the larvae. However, they will underestimate the power expended during locomotion.

After the first 30 h of development, lancelet larvae begin to locomote effectively using muscular body undulations. The energy expended during undulation is greater than that expended while ciliating (see Figs 12, 13). Comparable measurements of power for equally small undulating bodies are not available, although the power expended by a 5 cm long salmon was estimated to be 2.6×10^{-4} W (Webb, 1976*b*) and for a hovering 7 mm perch larva was 0.8×10^{-6} W (M. D. Stokes and J. R. Strickler, unpublished data). In comparison, the estimates for undulatory power in the larval lancelet, 10^{-6} to 10^{-9} W, are not unreasonable.

The Azuma (1992) model consistently predicted greater energy expenditure than did the Roberts (1981) undulatory model. Unfortunately, for undulatory motion at low Reynolds numbers, there is no simple comparative analogue similar to the inert sedimenting larva that can be used to the test the appropriateness of either model. Similarly, the differences in

the models that result from the choice of viscous drag coefficient cannot be tested. Even though the results appear to be reasonable, it will require a complete empirical description of the fluid flow around an undulating larva for comparison with theoretical models to test how accurately these different models estimate energy expenditure. Despite this, it is probably safe to assume that the energy expended during undulatory swimming is much higher than for ciliary swimming, particularly when realistic swimming speeds are used in the calculation.

Evolutionary considerations

Lancelet larvae have the ability to swim effectively using their body musculature by approximately 30 h after fertilization, once they are capable of propagating an undulating wave along the body, and the effectiveness of this locomotion increases rapidly thereafter. Even so, planktonic lancelet larvae spend most of their time hovering mid-water using their epidermal cilia even when they have the ability to undulate (Stokes and Holland, 1995*b*; Lacalli, 1996). As shown in Figs 12 and 13, the energetic cost of undulation is approximately an order of magnitude greater than that of ciliation. Larvae may hover predominantly because it conserves energy while permitting continuous filter feeding, thereby allowing the redirection of energy towards growth and development rather than locomotion. In addition to energy conservation, it has been postulated by some researchers (Paffenhöfer, 1983; Strickler, 1984) that movement can be 'noisy' and therefore might be more attractive to predators in the low Reynolds number realm. As illustrated in Fig. 11, undulation disrupts a larger volume of water than does ciliary swimming, in which energy is expended primarily within the cilia sublayer, and undulation therefore may produce a larger signal for predators to detect. However, the exact degree to which planktonic predators can utilize these signals needs further study. The difference in the fluid motion around ciliating *versus* undulating lancelet larvae is essentially the difference between those flows generated by an organism *tunnelling* through a very viscous medium as opposed to *pushing* against it.

The radical asymmetry of the lancelet larva has engendered considerable speculation (see Stokes and Holland, 1995*a*). Many authors have proposed larval asymmetry as an adaptation linked to the feeding process (e.g. van Wijhe, 1913; Garstang, 1928; Bone, 1958). Both van Wijhe (1927) and Gilmour (1994) have suggested that asymmetry provides an effective design for feeding while swimming along a rotating, spiral path. The observations in the present study suggest that this is not the case. A helical swimming path is most evident in larvae before feeding is initiated (see Fig. 3A), and planktonic larvae more than a few days old tend to hover almost motionless in the water column. In view of this, the structural arguments of Bone (1958), that the mouth has been displaced to the side of the body to maximize the size of the opening for effective filter feeding, seem more reasonable.

Lancelet larvae apparently have the nervous and muscular development necessary for undulatory locomotion at approximately 30 h post-fertilization. However, during their planktonic life, cilia-powered swimming predominates. It promotes feeding, is energetically less costly and may be less likely to attract predators than is undulation. Muscular body movements, in particular high-speed undulations, may be important as an escape response during planktonic life. Contemporary scenarios of vertebrate evolution include the shift from ciliary to undulatory locomotion as an important transitional step and have used locomotion in amphioxus as a recapitulation for this transition. This may be justified, but it is apparent that locomotory development in the larval lancelet is complicated by adaptations to their particular lifestyle, to hydrodynamic restrictions due to changes in the Reynolds number as they increase in size, and to constraints due to their morphological development.

I would like especially to thank J. Lawrence and D. Mahoney for providing laboratory facilities and equipment in Tampa Bay, Florida. Thanks to M. LaBarbera, P. Magwene and M. Hale for the use of high-speed video equipment and M. Latz and R. Shadwick for video support at SIO. I would also like to thank R. Emlet, J. Enright, N. Holland, S. Katz and G. Somero and two anonymous reviewers for constructive criticism of this manuscript. The work was funded in part by Research Grant No. RT 160-S from the Academic Senate of the University of California at San Diego.

References

AZUMA, A. (1992). *The Biokinetics of Flying and Swimming.* New York: Springer-Verlag. 283pp.

BAATRUP, E. (1981). Primary sensory cells in the skin of amphioxus (*Branchiostoma lanceolatum* (P)). *Acta Zool.* **62**, 147–157.

BATTY, R. S., BLAXTER, J. AND BONE, Q. (1991). The effect of temperature on the swimming of a teleost (*Clupea harengus*) and an ascidian larva (*Dendrodoa grassularia*). *Comp. Biochem Physiol.* **100** A, 297–300.

BEMS, W. E. AND GRADE, L. (1992). Early development of the Actinopterygian head. I. Observations on the external development and staging of the paddlefish, *Polyodon spathula*. *J. Morph.* **213**, 47–83.

BERGSTROM, J. (1989). The origin of animal phyla and the new phylum Procoelomata. *Lethaia* **22**, 259–269.

BERRILL, N. J. (1955). *The Origin of the Vertebrates.* Oxford: Clarendon Press. 257pp.

BLAKE, J. R. AND SLEIGH, M. A. (1974). Mechanics of ciliary locomotion. *Biol. Rev.* **49**, 85–125.

BLAXTER, J. H. (1969). Development: eggs and larvae. In *Fish Physiology*, vol. 3 (ed. W. S. Hoar and D. J. Randall), pp. 177–252. New York: Academic Press.

BLIGHT, A. R. (1976). Undulatory swimming with and without waves of contraction. *Nature* **264**, 352–354.

BLIGHT, A. R. (1977). The muscular control of vertebrate swimming movements. *Biol. Rev.* **52**, 181–218.

BONE, Q. (1958). Observations upon the living larva of amphioxus. *Pubbl. Staz. zool. Napoli* **30**, 458–471.

BONE, Q. (1992). On the locomotion of ascidian tadpole larvae. *J. mar. biol. Ass. U.K.* **72**, 161–186.

BONE, Q. AND BEST, A. C. G. (1978). Ciliated sensory cells in amphioxus (*Branchiostoma*). *J. mar. biol. Ass. U.K.* **58**, 479–486.

BOOTS, B. N. AND GETIS, A. (1988). *Point Pattern Analysis. Scientific Geography Series*, vol. 8 (series ed. G. I. Thrall). Boston: Sage Publications. 93pp.

BOSCHUNG, H. (1983). A new species of lancelet, *Branchiostoma longirostrum* (ORDER Amphioxi), from the western north atlantic. *Northeast Gulf Science* **6**, 91–97.

BOSCHUNG, H. AND GUNTER, G. (1966). A new species of lancelet, *Branchiostoma bennetti* (ORDER Amphioxi), from Louisiana. *Copeia* **1966**, 485–489.

BUDGETT, J. S. (1901). On the breeding habits of some West-African fishes. *Trans. zool. Soc. Lond.* **16**, 115–136.

CHIA, F., BUCKLAND-NICKS, J. AND YOUNG, C. M. (1984). Locomotion of marine invertebrate larvae: a review. *Can. J. Zool.* **62**, 1205–1222.

CHIN, T. G. (1941). Studies on the Amoy amphioxus *Branchiostoma belcheri* Gray. *Philip. J. Sci.* **75**, 369–421.

COGHILL, G. E. (1908). The development of the swimming movement in amphibian embryos. *Anat. Rec.* **2**, 148.

COX, R. G. (1970). The motion of long, slender bodies in viscous fluids. Part 1. General theory. *J. Fluid Mech.* **44**, 791–810.

EMLET, R. B. (1990). Flow fields around ciliated larvae: effects of natural and artificial tethers. *Mar. Ecol. Prog. Ser.* **63**, 211–225.

EMLET, R. B. (1994). Body form and function of ciliation in nonfeeding larvae of echinoderms: functional solutions to swimming in the plankton? *Am. Zool.* **34**, 570–585.

FETCHO, J. R. (1992). The spinal motor system in early vertebrates and some of its evolutionary changes. *Brain Behav. Evol.* **40**, 82–97.

FLOOD, P. R. (1975). Fine structure of the notochord of amphioxus. *Symp. zool. Soc. Lond.* **36**, 81–104.

FUIMAN, L. A. AND WEBB, P. W. (1988). Ontogeny of routine swimming activity and performance in zebra danios (Teleostei: Cyprinidae). *Anim. Behav.* **36**, 250–261.

GANS, C. (1989). Stages in the origin of vertebrates: analysis by means of scenarios. *Biol. Rev.* **64**, 221–268.

GANS, C. (1993). Evolutionary origin of the vertebrate skull. In *The Skull, Patterns of Structural and Systematic Diversity*, vol. 2 (ed. J. Hanken and B. K. Hall), pp. 1–35. Chicago: University of Chicago Press.

GARSTANG, W. (1928). The morphology of the Tunicata and its bearings on the phylogeny of the Chordata. *Q. J. microsc. Sci.* **72**, 51–187.

GILMOUR, T. H. J. (1994). Feeding methods of cephalochordate larvae. *J. Morph.* **220**, 349.

GRAY, J. AND HANCOCK, G. J. (1955). The propulsion of sea urchin spermatozoa. *J. exp. Biol.* **32**, 802–814.

GREENWOOD, P. H. (1958). Reproduction in the East African lungfish, *Protopterus aethiopicus* Haeckel. *Proc. zool. Soc. Lond.* **30**, 547–567.

GRIEG-SMITH, P. (1957). *Quantitative Plant Ecology*. London: Butterworth and Co. 256pp.

GUTHRIE, D. M. (1967). Control of muscular contractions by spinal neurones in amphioxus (*Branchiostoma lanceolatum*). *Nature* **216**, 1224–1225.

GUTHRIE, D. M. (1975). The physiology and structure of the nervous system of amphioxus (the lancelet), *Branchiostoma lanceolatum* Pallas. *Symp. zool. Soc. Lond.* **36**, 43–80.

GUTHRIE, D. M. AND BANKS, J. R. (1970). Observations on the function and physiological properties of a fast paramyosin muscle – the notochord of Amphioxus (*Branchiostoma lanceolatum*). *J. exp. Biol.* **52**, 125–138.

GUTMANN, W. F. (1981). Relationships between invertebrate phyla based on functional–mechanical analysis of the hydrostatic skeleton. *Am. Zool.* **21**, 63–81.

HAPPER, J. AND BRENNER, H. (1983). *Low Reynolds Number Hydrodynamics.* Boston: Martinus Nijhoff Publishers. 553pp.

HOLLAND, L. Z., PACE, D. A., BLINK, M. L., KENE, M. AND HOLLAND, N. D. (1995). Sequence and expression of amphioxus alkali myosin light chain (AmphiMLC-alk) throughout development: implications for vertebrate myogenesis. *Dev. Biol.* **171**, 665–676.

HOLLAND, N. D. AND HOLLAND, L. Z. (1994). Embryos and larvae of invertebrate deuterostomes. In *Essential Developmental Biology: a Practical Approach* (ed. C. Stern and P. W. H. Holland), pp. 21–32. Oxford: IRL Press.

HOLWILL, M. E. (1974). Hydrodynamic aspects of ciliary and flagellar movement. In *Cilia and Flagella* (ed. M. A. Sleigh), pp. 143-176. London: Academic Press.

HOLWILL, M. E. (1977). Low Reynolds number undulatory propulsion in organisms of different sizes. In *Scale Effects in Animal Locomotion* (ed. T. J. Pedley), pp. 233–242. London: Academic Press.

HUBBS, C. L. (1922). A list of the lancelets of the world with diagnoses of five new species of *Branchiostoma. Occasional papers of the Museum of Zoology, University of Michigan*. **105**, 1–16.

HUNTER, J. R. (1981). Feeding ecology and predation in marine fish larvae. In *Marine Fish Larvae* (ed. R. Lasker), pp. 33–79. Seattle: University of Washington Press.

INSOM, E., PUCCI, A. AND SIMONETTA, A. M. (1995). Cambrian protochordata, their origin and significance. *Boll. Zool.* **62**, 243–252.

JORDAN, C. E. (1992). A model of rapid-start swimming at intermediate Reynolds number: undulatory locomotion in the chaetagnath *Sagitta elegans*. *J. exp. Biol.* **163**, 119–137.

KELLER, S. R. AND WU, T. Y. (1977). A porous prolate-spheroidal model for ciliated micro-organisms. *J. Fluid Mech.* **80**, 257–278.

KEMP, A. (1996). Role of epidermal cilia in development of the Australian lungfish, *Neoceratodus forsteri* (Osteichthyes, Dipnoi). *J. Morph.* **228**, 203–221.

KIMMEL, C. B. (1993). Patterning the brain of the zebrafish embryo. *A. Rev. Neurosci.* **16**, 707–732.

KNIGHT JONES, E. W. (1954). Relations between metachronism and the direction of culiary beat in metazoa. *Q. J. microsc. Sci.* **95**, 503–521.

KNIGHT JONES, E. W. AND MILAR, R. H. (1949). Bilateral asymmetry shown by the metachronal waves in protochordate gill slits. *Nature* **163**, 137–138.

KOWALEVSKY, A. (1867). Entwickelungsgeschichte des *Amphioxus lanceolatus*. *Mem. Acad. Imp. Sci. St-Petersb*. (Ser. VII) **11**, 1–17.

LACALLI, T. C. (1996). Frontal eye circuitry, rostral sensory pathways and brain organization in amphioxus larvae: evidence from 3D reconstructions. *Phil. Trans. R. Soc. Lond. B* **351**, 243–263.

LACALLI, T. C., HOLLAND, N. D. AND WEST, J. E. (1994). Landmarks in the anterior central nervous system of amphioxus larvae. *Phil. Trans. R. Soc. Lond. B* **344**, 165–185.

LIGHTHILL, M. J. (1975). *Mathematical Biofluiddynamics*, vol. 17. Philadelphia: S.I.A.M. Publications. 279pp.

LIGHTHILL, M. J. (1976). Flagellar hydrodynamics. The John von Neumann Lecture, 1975. *S.I.A.M. Review* 1976.

LEUCKART, R. AND PAGENSTECHER, A. (1858). Untersuchungen über neidere Seethiere, *Amphioxus lanceolatus*. *Arch. Anat. Physiol. Wissensch. Med*. **1858**, 558–569.

MACHEMER, H. (1972). Ciliary activity and the origin of metachrony

in *Paramecium*: effects of increased viscosity. *J. exp. Biol.* **57**, 239–259.

NAEF, A. (1926). Notizen zur Morphologie und Stammesgeschichte der Wirbeltiere. *Pubbl. Staz. Zool. Napoli* **7**, 299–333.

NAITOH, Y. AND SUGINO, K. (1984). Ciliary movement and its control in *Paramecium*. *J. Protozool.* **31**, 31–40.

PAFFENHÖFER, G. A. (1983). Vertical zooplankton distribution on the northeastern Florida shelf and its relation to temperature and food abundance. *J. Plank. Res.* **5**, 15–33.

PIELOU, E. C. (1974). *Population and Community Ecology*. New York: Gordon and Breach, Science Publishers, Inc. 424pp.

ROBERTS, A. M. (1981). Hydrodynamics of protozoan swimming. In *Biochemistry and Physiology of Protozoa*, vol. 4 (ed. M. Levandowsky and S. H. Hunter), pp. 6–64. New York: Academic Press.

ROBERTS, A. AND TUNSTALL, M. J. (1994). Longitudinal gradients in the spinal-cord of *Xenopus* embryos and their possible role in coordination of swimming. *Eur. J. Morph.* **32**, 176–184.

SCHULTE, E. AND RIEHL, R. (1977). Elektronenmikroskipische Untersuchungen an den Oralcirren und der Haut von *Branchiostoma lanceolatum*. *Helgoländer wiss. Meeresunt.* **29**, 337–357.

SILLAR, K. T. AND ROBERTS, A. (1993). Control of frequency during swimming in *Xenopus* embryos: a study on interneuronal recruitment in a spinal rhythm generator. *J. Physiol., Lond.* **472**, 557–572.

SLEIGH, M. A. (1989). Adaptations of ciliary systems for the propulsion of water and mucus. *Comp. Biochem. Physiol.* **94**A, 359–364.

SLEIGH, M. A. AND BLAKE, J. R. (1977). Methods of ciliary propulsion and their size limitations. In *Scale Effects in Animal Locomotion* (ed. T. J. Pedley), pp. 243–256. London: Academic Press.

SOKAL, R. R. AND ROHLF, F. J. (1981). *Biometry*. New York: W. H. Freeman

SONG, J. AND NORTHCUTT, R. G. (1991). Morphology, distribution and innervation of the lateral line receptors of the Florida gar, *Lepisosteus platyrhincus*. *Brain Behav. Evol.* **37**, 10–37.

STEINER, H. (1939). Die Lokomotion durch Flimmerbewegung bei Amphibienlarven. *Rev. suisse Biol.* **46**, 369–375.

STOKES, M. D. AND HOLLAND, N. D. (1995*a*). Embryos and larvae of a lancelet, *Branchiostoma floridae*, from hatching through metamorphosis: growth in the laboratory and external morphology. *Acta Zool. (Stockholm)* **76**, 105–120.

STOKES, M. D. AND HOLLAND, N. D. (1995*b*). Ciliary hovering in larval lancelets (=amphioxus). *Biol. Bull. mar. biol. Lab., Woods Hole* **188**, 231–233.

STRICKLER, J. R. (1984). Sticky water: A selective force in copepod evolution. In *Trophic Interactions within Aquatic Ecosystems* (ed. D. G. Meyers and J. R. Strickler), pp. 187–242. Boulder, CO: Westview Press.

SUGINO, K. (1993). Video and microorganisms. In *Video Techniques in Animal Ecology and Behaviour* (ed. S. D. Wratten), pp. 163–204. London: Chapman & Hall.

SUGINO, K. AND NAITOH, Y. (1988). Estimation of ciliary activity in *Paramecium* from its swimming path. *Seitai no Kaqaku* **39**, 485–490.

VAN MIER, P., ARMSTRONG, J. AND ROBERTS, A. (1989). Development of early swimming in *Xenopus laevis* embryos: mytomal musculature, its innervation and activation. *Neuroscience* **32**, 113–126.

VAN WIJHE, J. W. (1913). On the metamorphosis of *Amphioxus lanceolatus*. *Proc. Kon. Akad. Wetensch. (Sci. Sect.)* **16**, 574–583.

VAN WIJHE, J. W. (1925). On the temporary presence of the primary mouth-opening in the larvae of amphioxus and the occurrence of three postoral papillae, which are probably homologous with those of the larvae of ascidians. *Proc. K. Ned. Akad. Wet. Amsterdam* **29**, 286–295.

VAN WIJHE, J. W. (1927). Observations on the adhesive apparatus and the function of the ilio-colon ring in the living larva of amphioxus in the growth period. *Proc. Konin. Acad. Wet. Amsterdam* **30**, 991–1003.

VOGEL, S. (1981). *Life in Moving Fluids. The Physical Biology of Flow*. New Jersey: Princeton University Press. 352pp.

WARDLE, C. S., VIDELER, J. J. AND ALTRINGHAM, J. D. (1995). Tuning in to fish swimming waves: body form, swimming mode and muscle function. *J. exp. Biol.* **198**, 1629–1636.

WEBB, J. E. (1969). On the feeding and behaviour of the larvae of *Branchiostoma lanceolatum*. *Mar. Biol.* **3**, 58–72.

WEBB, J. E. (1973). The role of the notochord in forward and reverse swimming and burrowing in the amphioxus, *Branchiostoma lanceolatum*. *J. Zool., Lond.* **170**, 325–338.

WEBB, J. E. (1975). The distribution of *Amphioxus*. *Symp. zool. Soc. Lond.* **36**, 179–212.

WEBB, J. E. (1976*a*). A review of swimming in *Amphioxus*. In *Perspectives in Experimental Biology*, vol. 1, *Zoology* (ed. P. S. Davies), pp. 447–454. New York: Pergamon Press.

WEBB, P. W. (1976*b*). Hydrodynamics and energetics of fish propulsion. *Bull. Fish. Res.Bd Can.* **190**, 1–160.

WEBB, P. W. (1993). Swimming. In *The Physiology of Fishes*, pp. 47–43. London: CRC Press.

WEIHS, D. (1979). Energetic significance of changes in swimming modes during growth of larval anchovy, *Engraulis mordax*. *Fishery Bull. Fish. Wildl. Serv. U.S.* **77**, 597–604.

WHITING, H. P., BANNISTER, L. H., BARWICK, R. E. AND BONE, Q. (1993). Early locomotor behaviour and the structure of the nervous system in embryos and larvae of the Australian lungfish, *Neoceratodus forsteri*. *J. Zool., Lond.* **226**, 175–198.

WICKSTEAD, J. H. (1967). *Branchiostoma lanceolatum* larvae: some experiments on the effect of thiouracil on metamorphosis. *J. mar. biol. Ass. U.K.* **47**, 49–59.

WICKSTEAD, J. H. (1975). Chordata: Acrania (Cephalochordata). In *Reproduction of Marine Invertebrates*, vol. II, *Entoprocts and Lesser Coelomates* (ed. A. C. Giese and J. S. Pearse), pp. 282–319. New York: Academic Press.

WICKSTEAD, J. H. AND BONE, Q. (1959). Ecology of acraniate larvae. *Nature* **184**, 1849–1851.

WILLEY, A. (1891). The later larval development of amphioxus. *Q. J. microsc. Sci*. **32**, 183–234.

WILLEY, A. (1894). *Amphioxus and the Ancestry of the Vertebrates.* New York: Macmillan. 316pp.

WINET, H. (1973). Wall-drag on free-moving ciliated microorganisms. *J. exp. Biol.* **59**, 753–766.

WU, T. Y. (1977). Introduction to the scaling of aquatic animal locomotion. In *Scale Effects in Animal Locomotion* (ed. T. J. Pedley), pp. 203–232. London: Academic Press.

YOSHIDA, M., MATSUURA, K. AND UEMATSU, K. (1996). Developmental changes in the swimming behavior and underlying motoneuron activity in the larval angelfish, *Pterophyllum scalare*. *Zool. Sci.* **13**, 229–234.